

# Review of Curcumin Physicochemical Targeting Delivery System

This article was published in the following Dove Press journal:  
*International Journal of Nanomedicine*

Lanmei Li<sup>1,2,\*</sup>  
Xiaomei Zhang<sup>3,\*</sup>  
Chao Pi<sup>1</sup>  
Hongru Yang<sup>4</sup>  
Xiaoli Zheng<sup>5</sup>  
Ling Zhao<sup>1</sup>  
Yumeng Wei<sup>1</sup>

<sup>1</sup>Central Nervous System Drug Key Laboratory of Sichuan Province, School of Pharmacy, Southwest Medical University, Luzhou, Sichuan 646000, People's Republic of China; <sup>2</sup>Nanchong Key Laboratory of Individualized Drug Therapy, Department of Pharmacy, The Second Clinical Medical College of North Sichuan Medical College, Nanchong Central Hospital, Nanchong, Sichuan 637000, People's Republic of China; <sup>3</sup>Institute of Medicinal Chemistry of Chinese Medicine, Chongqing Academy of Chinese MateriaMedica, Chongqing 400065, People's Republic of China; <sup>4</sup>Department of Oncology of Luzhou People's Hospital, Luzhou, Sichuan 646000, People's Republic of China; <sup>5</sup>Basic Medical College of Southwest Medical University, Luzhou, Sichuan 646000, People's Republic of China

\*These authors contributed equally to this work

Correspondence: Ling Zhao; Yumeng Wei  
School of Pharmacy, Southwest Medical University, No. 3-319, Zhongshan Road, Jiangyang District, Luzhou City, Sichuan Province 646000, People's Republic of China  
Tel/Fax +86 830 3162292  
Email zhaoling-998@163.com; weiyumeng-268@163.com

**Abstract:** Curcumin (CUR), as a traditional Chinese medicine monomer extracted from the rhizomes of some plants in Ginkgo and Araceae, has shown a wide range of therapeutic and pharmacological activities such as anti-tumor, anti-inflammatory, anti-oxidation, anti-virus, anti-liver fibrosis, anti-atherosclerosis, and anti-Alzheimer's disease. However, some issues significantly affect its biological activity, such as low aqueous solubility, physico-chemical instability, poor bioavailability, and low targeting efficacy. In order to further improve its curative effect, numerous efficient drug delivery systems have been carried out. Among them, physicochemical targeting preparations could improve the properties, targeting ability, and biological activity of CUR. Therefore, in this review, CUR carrier systems are discussed that are driven by physicochemical characteristics of the microenvironment (eg, pH variation of tumorous tissues), affected by external influences like magnetic fields and vehicles formulated with thermo-sensitive materials.

**Keywords:** curcumin, targeted delivery system, pH-sensitive, magnetic-response, thermo-sensitive, cancer

## Introduction

Chemotherapy is the most commonly used method for advanced cancer. However, the clinical usefulness of chemotherapy drugs are still restricted by severe toxic and side-effects such as myelosuppression, immunologic suppression, gastrointestinal reaction, and peripheral neuropathy.<sup>1-5</sup> Some effective components of plants used in traditional medicine without the serious side-effects, as a supplementary treatment, have been widely studied.<sup>6,7</sup> Among them, Curcumin (CUR), a traditional Chinese medicine monomer, has been extensively studied with broad pharmacological activities, as summarized in Figure 1.<sup>8-10</sup> Its anti-tumor effect has been the most extensively studied and are related to regulating enzymes (COX-2, AMPK, MMPs, NADPH, and LOX), transcription factors (NF- $\kappa$ B, AP-1,  $\beta$ -catenin, and STAT-3) and protein kinases, growth factors (MAPK, AKT, JAK, VEGF, ERK, PKA, and Bcl-2), etc.<sup>11-13</sup> However, it still needs to be improved in many fields, including low aqueous solubility and physico-chemical stability, low absorption rate, rapid metabolism, low bioavailability, and targeting efficacy<sup>14,15</sup> These problems significantly affect its biological activity and application in the clinic.

In recent years, some novel targeted drug delivery systems have been favored by researchers, such as passive targeting preparations, active targeting preparations, and physicochemical targeting preparations. Passive targeting preparations are enriched in target sites through normal physiological processes to improve the curative effect, such

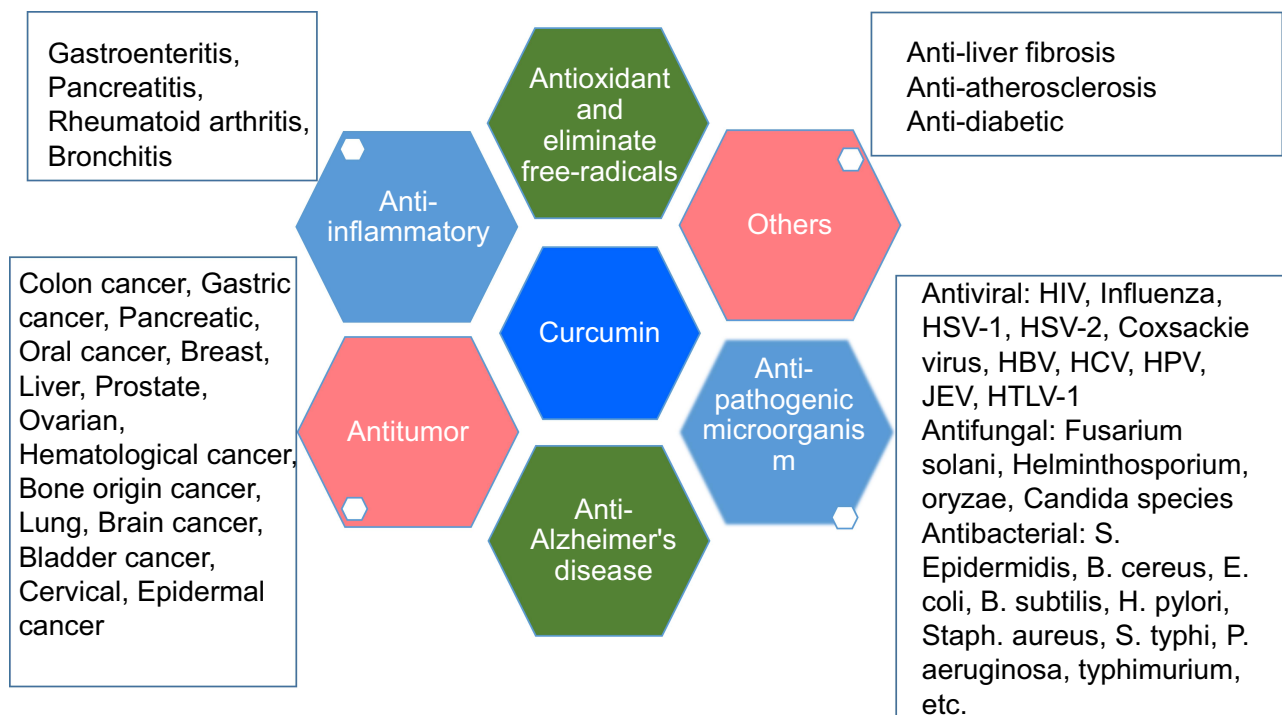


**Figure 1** Pharmacological activities of Curcumin.

**Abbreviations:** PIV-3, parainfluenza virus type 3; FIPV, feline infectious peritonitis virus; VSV, vesicular stomatitis virus; HSV, herpes simplex virus; FHV, flock house virus; RSV, respiratory syncytial virus; HIV-1, type 1 human immunodeficiency virus; HSV-1, herpes simplex virus type 1; HBV hepatitis B virus; HCV hepatitis C virus; HPVs, high-risk human papillomaviruses; JEV, Japanese encephalitis virus; HTLV-1, human T-cell leukemia virus type 1.

as liposomes, nanoparticles, emulsions, microcapsules, microspheres, and micelles.<sup>16-20</sup> Although it was a potential method to solve the above problems of CUR to a certain degree,<sup>16,21-24</sup> it is easy to be swallowed by macrophages in the body leading to drug accumulation in the liver, spleen, and kidney tissues.<sup>25</sup> In a word, passive targeting preparations are non-intelligent and non-specific for drug delivery. Successful development of targeted therapy is dependent on the site-specific delivery of therapeutic agents partly. Active targeting preparations as “missiles” deliver drugs to target areas by modifying specific ligands or monoclonal antibodies on particle surfaces to avoid the uptake of the reticuloendothelial system and drug natural distribution.<sup>26</sup> However, these active targeting preparations have several limitations such as complicated preparation procedures, non-specific tumor targeting, and single target properties that are only targeted to a certain receptor or ligand.<sup>27-29</sup> Recent studies showed that physicochemical targeting preparations such as pH-, magnetic-, and heat-response proved to be promising strategies to obtain controllable and specific drug delivery (Figure 2). Among them, specific release behavior of pH sensitive preparations was triggered by the specific pH of the target site to increase target ability,<sup>30</sup> especially in the acidic environment of tumor

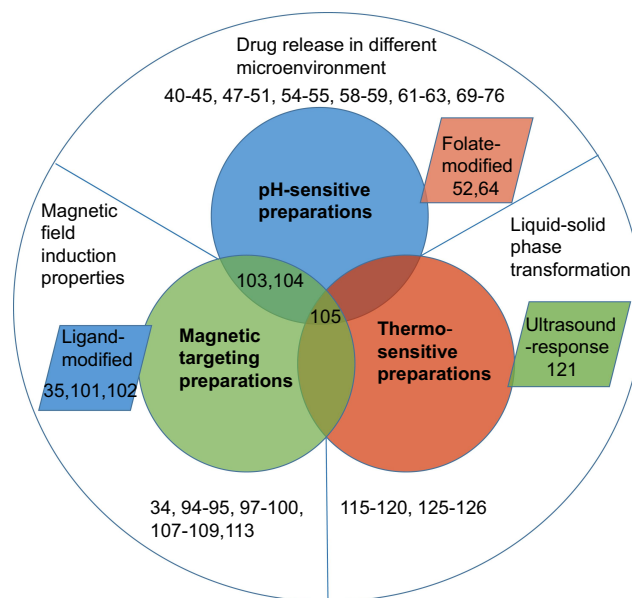


**Figure 2** Physicochemical targeting preparations of Curcumin.

tissues.<sup>31</sup> In consideration of tissue microenvironment, pro-drug or carriers-modified design was reported for enhancing the antitumor effect by selectively transporting drugs to targets.<sup>32</sup> Magnetic-response preparations could deliver drugs to specific target areas through blood vessels under the

guidance of strong external magnetic fields.<sup>33</sup> Magnetic-response drug delivery systems could improve serum bioavailability of CUR in mice up to 2.5-fold through delayed-metabolism and increased accumulation *in vivo*.<sup>34</sup> When CUR-loaded magnetic nanoparticles combined with ligand/receptor, serving as novel platforms for multiple biomedical applications, they could enhance the targeting and cellular uptake ability, leading to an improved anticancer effect.<sup>35</sup> Besides, this combination also achieved controllable and specific drug delivery through thermo-sensitive targeting preparations by temperature stimuli.<sup>36</sup> Generally, these physicochemical targeting preparations could enhance the properties of CUR such as targeting ability, aqueous solubility, stability, bioavailability, and therapy effect (anti-tumor, anti-inflammatory, and antioxidant activity), as shown in Table 1. This review mainly focuses on different formulations containing CUR based on physicochemical properties of carriers and their pharmaceutical properties.

## pH-Sensitive Preparation

To increase the accumulation of drugs in the target tissues or cells, different trigger release mechanisms have been designed based on the body microenvironment, especially the tumor microenvironment. The different microenvironment of tumors from that of normal tissues is largely dictated by the abnormal tumor vasculature and heterogeneous microcirculation. Its hostile microenvironment, such as oxygen consumption, glucose, and energy deficiency, high lactate level and extracellular acidosis, causes the accumulation of acid metabolites resulting in the extracellular matrix of tumor tissue being acidic, and its pH (about 6.5–7.2) is lower than that of blood and normal tissue (7.4).<sup>37</sup> A study demonstrated that pH-sensitive drug delivery systems could increase drug accumulation in the tumor, enhance the cellular uptake ability and improve antitumor activity in weakly acidic conditions.<sup>32</sup> Due to the pH-response property, drugs were also delivered to the inflammatory regions and infected areas.<sup>30,31</sup> In addition, in view of specific normal physiological microenvironments such as intestinal fluid (SIF, pH 6.8) and simulated gastric fluid (SGF, pH 1.2),<sup>38</sup> drug delivery systems for the gastrointestinal tract have also been developed.<sup>39</sup> Based on the different acidity/alkalinity microenvironment of the body for any situation, physiological or pathological, various CUR pH-sensitive preparations (liposomes, nanoparticle, micelles, microspheres) were developed to enhance the targeting ability and treatment effect of CUR (Figure 3).

## CUR pH-Sensitive Liposomes

Lipid carriers as pH-sensitive materials, responding to acidic condition of tumors or inflammation regions, are used to load CUR achieving intelligent release of drug, as shown in Table 2. This drug delivery platform could enhance the anti-tumor and anti-inflammatory effect of lipophilic CUR. For example, the pH-sensitive material of IM-Chol was synthesized through amidation reaction between the amino group of N-(3-Aminopropyl) imidazole and acyl chloride group of cholesteryl chloroformate in a weak base solution, which were used to prepare CUR pH-sensitive liposomes with phosphatidylcholine and cholesterol by thin-film dispersion method (Figure 3). The cumulative release of CUR (72.5%) after 24 hours at pH 5.0 were higher than that at pH 7.4 (32%), indicating that IM-Chol displayed a pH-response property. The cell toxicity result showed an enhanced inhibitory effect on EC109 cells with the cell viability of 30% compared with free CUR (60%).<sup>40</sup> An endosomal pH-sensitive cationic lipid, consisting of glutamic acid backbone-based cationic amphiphiles that contain both endosomal pH-sensitive histidine and solubility enhancing guanidine moieties in their polar head-group regions, was used to encapsulate CUR for targeting therapy of the tumor. CUR release from the liposomes was most efficient at pH 5 or 6. And it showed a burst release in the first 1 hour followed by a controlled release over a period of 4 hours (85%). Importantly, the concentrations of CUR liposome in the tumor tissues were found to be remarkably higher than those in other tissues such as the lung, liver, kidney, spleen, and heart. The tumor volume of CUR liposome (about 800 mm<sup>3</sup>) and the vehicle control group (5% aqueous glucose) (about 4,200 mm<sup>3</sup>) revealed that CUR was effectively transported to mouse (C57BL/6 mice bearing) tumors and significantly contributed to inhibiting mouse tumor growth. The survival rate of tumor bearing mice with treatment of CUR liposome (about 45 days) was also improved compared to the control group (about 32 days).<sup>41</sup> Besides, some non-lipid carriers as pH-sensitive materials have been reported to entrap CUR. For example, the pH-sensitive material of pI-pAA (2.5 mol%) and these carriers of dipalmitoylphosphatidylcholine/cholesterol (2:1 M ratio) and polyoxyethylated calix-4-arene (phospholipids/CUR, 1/0.1 M ratio) were used to obtain the CUR-loaded pH-sensitive liposomes by lipid film hydration method and extrusion. The liposomes showed a superior cytotoxic and apoptogenic activity against chemo-sensitive HL-60

**Table 1** The Influential Effect and Preparation Method of CUR-Loaded Physicochemical Targeting Preparations

Preparations	Influential Effects	Preparation Method	Size	Ref.
pH-sensitive				
Liposome	Enhanced inhibitory effect on EC109 Effectively transported to mouse (C57BL/6 mice bearing) tumor and significantly inhibited mouse tumor growth Superior cytotoxic activity and proapoptotic against both HL-60 and HL-60/CDDP cells Anti-inflammatory and antioxidant activity in vitro	Thin-film dispersion	141 nm	40
		Ultrasonic film hydration	193 nm	41
		Lipid film hydration method and extrusion	127 nm	42
		Micellar-vesicle transformation method and pH-driven method	<100 nm	43
Nanoparticle	1) Efficiently penetrate the blood–brain barrier and enhance brain delivery efficiency; 2) Increase mouse survival rate and reduce adverse reactions Colonic specific drug release  Enhanced permeation across Caco-2 cell and significantly decreased neutrophil infiltration and TNF- $\alpha$ secretion  Double inhibition of the cancerous cells  Significantly released at pH 7.0 Enhanced significant cytotoxicity against MRC5 cells  Delivered effectively drug to tumor and improved targeting ability	Single-emulsion solvent evaporation method	100 nm	35
		Solvent emulsion evaporation technique	111 nm	44
		Modified spontaneous emulsification solvent diffusion method	116 nm	46
		Solvent emulsion-evaporation technique	97 nm	47
		Ionic-gelation method	173 nm	48
		Rotary evaporation and deposition coating	234 nm	50
		Co-condensation and coated method	about 80 nm	51
Micelle	Increased the tumor inhibition for HeLa, SiHa, and C33a cervical cell lines Extended the MRT and delayed the clearance of CUR Inhibited tumor growth and exert MDR Release rapidly CUR at the acidic environment	Dialysis method	95 nm	57
		Solvent evaporation method	143 nm	58
		Synthesis and self-assemble	228 nm	60
		Synthesis and self-assemble	222 nm	61
Microsphere	1) Prevented premature release and controlled release; 2) Significantly reduced severity of colonic damage	Emulsion cross-linking method followed by coating	77 nm	66
Molecular complexes	1) Enhanced the aqueous solubility (>2 mg/mL); 2) Increased peak plasma concentration (6 times); 3) Improved bioavailability (about 20-fold)	Nanoprecipitation method	-	67
Microcapsule	Suppressed degradation of CUR and controlled drug release	Synthesis and self-assemble	1.05 $\mu$ m	68
Magnetic-response				
Nanoparticle	1) Suppressed of PCNA, Bcl-xL, Mcl-1, MUC1, Collagen I and enhanced membrane $\beta$ -catenin expression; 2) Improved serum bioavailability (2.5-fold) Sustained-release Showed high stability, well-tolerated by mammalian cells and MRI relaxation properties Displayed strong anticancer on MDA-MB-231 cancer cells and superior magnetic resonance imaging characteristics	Water-dispersible multi-layer synthesis approach	10.5 $\pm$ 0.54 nm	34
		Modified co-precipitation	100 nm	87
		Ultrasonic dispersion and incubation chelation method	13 $\pm$ 4 nm	91
		Modified co-precipitation and injection method	123 nm	92
Functional particle	Significantly enhanced the cellular uptake and better antiproliferative effect on the C6 glioma cell and HeLa cells	Co-precipitation, dispersion and synthesis methods	117 nm	94

(Continued)

**Table 1** (Continued).

Preparations	Influential Effects	Preparation Method	Size	Ref.
	1) pH sensitive release, high loading capacity and hemocompatibility of CUR; 2) Enhanced uptake and antiproliferation for MCF-7 breast cancer cell	Chemical co-precipitation method and molecular modified	195 and 240 nm	95
	1) improved the solubility (216 µg/mL), stability and bioavailability of CUR; 2) Suppressed the growth of Caco-2 cells (CC50=65 µg/mL)	Ice bath sonication and precipitation method	10 µm	97
Liposome	Magnetic heating controlled drug release by high-frequency magnetic field exposure; efficiently internalized into the cellular compartment and killed MCF-7 cells	Thin-film hydration method followed by extrusion techniques	120–140 nm	99
Microsphere	Showed controllable particle size and possessed good magnetic mobility  Induced HeLa cancer cells death through magnetocaloric effect	Water-in-oil-in-water method	16–207 µm	100
		Solvent evaporation method	75 nm	101
Hydrogel	Cardioprotective effects against dox-induced cardiac toxicity in rat cardiomyocyte cell lines	Emulsion polymerization and synthesis method	18–23 nm	105
Thermo-sensitive				
Polymer gel	Improved targeting and bioavailability in the brain Temperature controlled release performance Significantly prolong retention time in solid tumors	Solvent injection method	–	108
		Emulsion polymerization	180 nm	109
		Solvent injection method	-	110
Liposomal-based gel	Showed better skin permeation in vitro and significant anti-inflammatory effect in auricle edemas mice  Reduced toxicity of CUR and enhanced anti-tumor activity in tumor-bearing BALB/c mice	Emulsion evaporation-solidification at low temperature	263.9 nm	112
		Thin-film rehydration method	950 nm	113
Micelle-based gel	1) Inhibited tumor growth and metastasis, and prolonged survival of tumor-bearing mice; 2) Showed lower proliferation activity, more apoptotic cells, and fewer microvessels; 3) Showed higher AUC and longer t1/2.  Showed nano-scale size, low critical micelle concentration (0.0113–0.0144 mg/mL), high drug loading (20.4%) and stability (remain stable over 1 month)	Dispersion method	27.1 nm	117
		Self-assembly and solvent evaporation/film hydration method	47.5–88.2 nm	118

**Abbreviation:** CUR, curcumin.

and its resistant sublines HL-60/doxorubicin (Dox).<sup>42</sup> Eudragit<sup>®</sup>S100, made of methacrylic acid and methacrylic acid methyl ester, was used to coat the surface of CUR-loaded liposomes for colon targeted therapy due to its pH-dependent solubility in the colon region. Vincenzo et al<sup>43</sup> prepared CUR-loaded liposomes in a simple and organic solvent-free way by a micellar-vesicle transformation method and coated with Eudragit<sup>®</sup> S100 on its surface by a fast pH-driven method, as shown in Figure 4. The liposomes have small particle size (<100 nm), high encapsulation efficiency (98%), and high stability at both 4°C and 25°C. The cytotoxicity experiment of the liposomes showed safety on the Caco-2 human colon cell line

in vitro. These drug delivery systems showed good characteristics such as intelligent drug release behavior and improved stability. However, the study of pharmacokinetics is important for the application of CUR in the clinic and needs to be carried out.

## CUR pH-Sensitive Nanoparticles

Many CUR-loaded pH-sensitive nanoparticles were developed for oral colon-specific drug delivery systems (OCDDS), which could release drug under neutral conditions. This system has proved safety, good targeting property for colonic lesions, controlled/sustained release, and better therapeutic efficacy. As mentioned above,

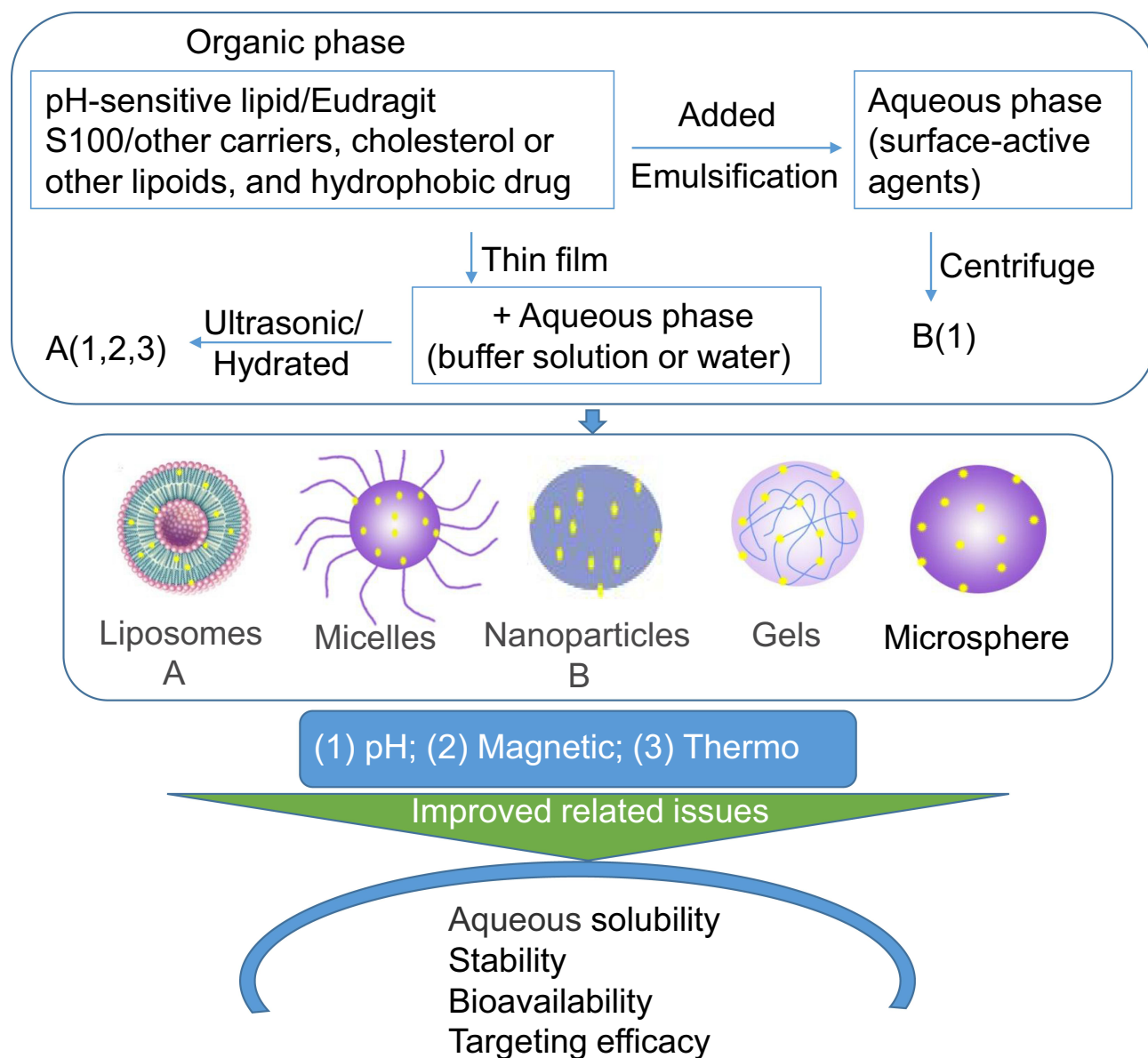


**Figure 3** Schematic transition of CUR into physicochemical targeting preparations.

Eudragit<sup>®</sup>S100, as a good pH-sensitive carrier, could selectively release drug at the colon region rather than in the stomach and upper intestine due to the ionization of its carboxylic functional group at pH 7.0.<sup>44</sup> Eudragit<sup>®</sup>S100 showed good security for oral administration. CUR-loaded polymeric nanoparticles with Eudragit<sup>®</sup>S100 showed no toxicity evidenced by various toxicological evaluations including acute-toxicity study (at a dose equivalent to 2,000 mg/kg CUR), 28 days sub-acute-toxicity study (200 mg/kg CUR) and various genotoxicity studies (micronucleus assay, chromosomal aberration assay, and comet assay in vivo).<sup>45</sup> In 1978, it was reported for the

first time that after oral administration of CUR (1 g/kg) in Sprague-Dawley rats, negligible amounts of CUR were observed in blood plasma which could be its poor absorption from the gut.<sup>46</sup> When CUR was encapsulated into pH-sensitive nanoparticles, it exhibited better permeation and selective release of drug in the inflamed colonic tissues. The CUR-loaded pH-sensitive nanoparticles (CUR-loaded NPs) consisting of PLGA (poly(lactic-co-glycolic) acid, 45 mg), Eudragit<sup>®</sup>S100 (45 mg), and PVA solution (polyvinyl alcohol, 0.5%, w/v) could enhance the permeation across Caco-2 cells monolayers. The apparent permeability ( $P_{app}$ ) of the CUR-loaded NPs was about  $2.6 \times 10^{-6}$  cm/

**Table 2** The Trigger/Targeting Carries and Preparation Method of CUR-Loaded Physicochemical Targeting Preparations

Types	Trigger/Targeting Carries	Ref.
pH-sensitive	1) N-(3-Aminopropyl)imidazole-cholesterol (IM-Chol)	40
	2) A new endosomal cationic lipid consisted of glutamic acid backbone-based cationic amphiphiles	41
	3) Poly(isoprene-b-acrylic acid) copolymer (pl-pAA)	42
	4) Eudragit®S100	43–47,66
	5) Chitosan and fucoidan	48
	6) Functionalized dendritic mesoporous silica	49
	7) Tannic acid-Fe(III) complex	50
	8) Chitosan and folate	51
	9) D- $\alpha$ -tocopheryl polyethylene glycol 1000-block-poly( $\beta$ -amino ester) (TPGS-PAE copolymers)	52
	10) PEG <sub>2000</sub> -DOX	53
	11) Dox-oxidized sodium alginate (Dox-OSA)	54
	12) Zn(II)-CUR	55
	13) Amphiphilic N-benzyl-N,O-succinyl chitosan (BSCS)	57
	14) Poly(3-caprolactone)-block-poly(diethylaminoethyl methacrylate)-block-poly(sulfobetaine methacrylate) (PCL-PDEA-PSBMA)	58,59
	15) Poly(l-histidine)-poly(D,L-lactide-co-glycolide)-poly(ethylene glycol)-poly(D,L-lactide-co-glycolide)-poly(l-histidine) (PHis-PLA-PEG-PLA-Phis) and a folate targeting ligand	60
	16) CUR-dextran	61
	17) Poloxam 188-Cis-CUR conjugate	62
	18) mPEG-poly(lactic acid)-CUR and mPEG-poly(lactic acid)-hydrazone-CUR (mPEG-PLA-CUR and mPEG-PLA-Hydr-CUR)	63
	19) mPEG-PLA-tris(hydroxymethyl)aminomethane-CUR (mPEG-PLA-Tris-CUR)	64
	20) mPEG-Chitosan-Ketal (PCK)	65
	21) Poly(butyl-methacrylate-co-(2-dimethylaminoethyl) methacrylate-co-methyl-methacrylate) (Eudragit® EPO)	67
	22) Silica particles and poly(L-lysine)	68
	23) $\beta$ -CD	96
	24) Pectin maleate	97
Magnetic	1) Oleic acid-modified iron oxide nanoparticles and NH <sub>2</sub> -PEG <sub>3500</sub> -T7	35
	2) Magnetic ferrite	34,85–87,89–97,99–102,105
Thermo-sensitive	1) N-isopropyl acrylamide	97
	2) Poloxamer 407	107,108,110–112
	3) Poly(N-vinylcaprolactam-co-hydroxyl ethyl ethacrylate)	109
	4) N-cholesteryl hemisuccinate-O-sulfate chitosan	113
	5) Poly(ethylene glycol)-poly( $\epsilon$ -caprolactone)-poly(ethylene glycol) copolymer	117
	6) Poly(N-isopropylacrylamide-co-N,N-dimethylacrylamide)-b-poly(L-lactide)-b- poly(N-isopropylacrylamide-co-N,N-dimethylacrylamide)	118

**Abbreviations:** CUR, curcumin; T7, human transferrin receptor-binding peptide T7.

s, while that of CUR suspension was undetectable. Furthermore, CUR-loaded NPs showed a significant reduction on TNF- $\alpha$  secretion against J774 macrophage cell lines. The amount of TNF- $\alpha$  in the untreated group, CUR suspension and CUR-loaded NPs-treated cells was about 1,800, 1,400, and 510 pg/mL, respectively. CUR was not released in the medium at pH 1.2 or 4.5 (<15%), but was rapidly released at neutral pH values.<sup>47</sup> Other CUR pH-sensitive nanoparticles were prepared by solvent

emulsion-evaporation technique with CUR (10 mg), Eudragit®S100 (10 mg), TPGS (d- $\alpha$ -tocopheryl polyethylene glycol 1000 succinate, 0.05%, w/v) and PVP K-90/D (poly vinyl pyrrolidone, 0.075%, w/v) (Figure 3). It showed the superior cytotoxic action against HT-29 cells compared with free CUR (IC<sub>50</sub>, 5 vs 50  $\mu$ M).<sup>48</sup> However, its pharmacokinetics and therapy effect in vivo needs further study, which could be due to the extremely pronounced instability, and there are a number of

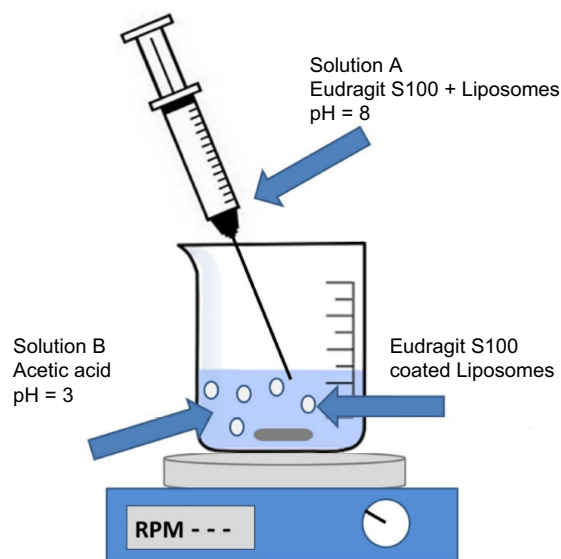


**Figure 4** Schematic representation of liposomal coating with Eudragit® S100 by the pH jump method.

**Notes:** Reprinted with permission from De LV, Milano F, Mancini E, et al. Encapsulation of curcumin-loaded liposomes for colonic drug delivery in a pH-responsive polymer cluster using a pH-driven and organic solvent-free process. *Molecules*. 2018;23(4):739. Copyright (2018) Multidisciplinary Digital Publishing Institute, Creative Common CC BY license.<sup>43</sup>

prospective failures in determination of CUR content. Besides, Chitosan/Fucoidan was used to control release of CUR due to the ionization and deprotonation of the amino groups ( $-\text{NH}_3^+$ ) on chitosan and the sulfate groups ( $-\text{SO}_3^-$ ) on fucoidan for overcoming the barriers to the gastrointestinal (GI) tract. The chitosan/fucoidan nanoparticles, consisting of chitosan (5 mg), fucoidan (5 mg) and acetic acid (0.01%, v/v), showed representative pH-dependent sustained release behavior. The release of CUR was inhibited at pH 1.2 ( $<15 \mu\text{g/mL}$ , after 12 hours), but significantly rose at pH 7.0 (about  $22.5 \mu\text{g/mL}$ ).<sup>49</sup>

CUR pH-sensitive nanoparticles were developed for controlled drugs release in acidic or weak acidic conditions. Various nanostructured-mesoporous silica materials (MSMs) were modified with the functional group such as  $-\text{NH}_2$  and silanol groups for controlled release of CUR. Both MCM-41 (well-known 2D silica material) and KKC-1 (present unique new 3D fibrous-structured silica) were functionalized with aminopropyl groups to obtain MCM- $\text{NH}_2$  (two dimensional) and KCC- $\text{NH}_2$  (three dimensional). The nanoparticles containing MCM- $\text{NH}_2$  or KCC- $\text{NH}_2$  could achieve controlled, long-term and effective pH-stimulated release of CUR. The cumulative release rates of CUR from silica materials during 100 hours were about 14% in the case of MCM- $\text{NH}_2$  and about 19% in the

case of KCC- $\text{NH}_2$  at pH 2.5, while they were only about 5.5% and 14% under neutral pH conditions (pH 7.5), respectively. As shown in the study of Abouaitah et al,<sup>50</sup> the CUR-loaded functionalized dendritic mesoporous silica nanoparticles under low acidic condition (pH 2–5) exhibited positive charge, while under neutral pH condition ( $\sim 7.5$ ) was negative. It indicated that the enhanced cumulative release is contributed to the protonation of the  $-\text{NH}_2$  groups on the surface of silica nanoparticles under low pH condition. Mesoporous silica nanoparticles (MSNs) with tannic acid (TA)-Fe(III) complex deposited on its surface showed pH- and glutathione-responsive drug release. The CUR release from tannic acid-Fe(III) coated MCM-41 was significantly decreased compared to non-coated MCM-41. At pH values lower than 2, only the mono-complex TA can be formed, while at pH values higher than 7, three moieties of tannic acid are strongly bonded to Fe(III). The zeta potential values increase as pH value decreases from 7.4 to 4.0, because of the protonation of silanol groups of the silica surface. Thus, on the one hand, the rapid release of CUR was triggered by weak acid condition (pH 6.0 or 4.5), but sustainable drug release was shown under physiological conditions (pH 7.4). On the other hand, the glutathione concentrations of some cancer tissues could be 4-fold higher than normal tissues, and its concentration interior of the cells is significantly higher than the extracellular. Thus, the drug release could be controlled for the level of glutathione as a good ligand for Fe(III) ions which accelerated the decomposition of the TA-Fe(III) complex. The resulting dual-responsive drug delivery system could significantly enhance cytotoxicity against MRC5 cells. The  $\text{IC}_{50}$  of free CUR and the dual-responsive system were  $>150 \mu\text{M}$  and  $20.2 \pm 3.5 \mu\text{M}$ , respectively.<sup>51</sup> Therefore, this dual sensitive drug delivery system has great potential for tumor targeted therapy. Other MSNs were functionalized with (3-aminopropyl) triethoxysilane to obtain amine functionalized MSNs, then conjugated with succinic anhydride to obtain carboxylic acid functionalized MSNs (MSN-COOH) for encapsulating CUR, and lastly coated with chitosan-folate via electrostatic interaction on its surface. The CUR loading efficiency ( $\text{CLE}=31.2\%$ ) and loading capacity ( $\text{CLC}=4.6\%$ ) of MSNs with mesitylene as the swelling agent (LMSN-COOH-CUR) is 2-fold higher than that without mesitylene. It could be attributed to the fact that the decrease in the pore size of MSNs led to a drop in CLE and CLC. The CUR-loaded chitosan-folate coated mesoporous silica nanoparticles (LMSN-COOH-CUR@CS-FA)



showed pH-sensitive drug release behavior. At pH 5.5, the release is significantly faster than pH 7.4. It could be due to the high permeability and swelling ability of chitosan at acidic environments. Cellular uptake studies showed that free CUR were more effective in penetrating both cell lines (HeLa and NIH-3T3) than CUR loaded MSNs.<sup>52</sup> It could be attributed to the hydrophobic nature of CUR as a small molecule material which can easily diffuse through phospholipid cell membrane.<sup>53</sup> The higher cellular uptake of LMSN-COOH-CUR@CS (more positive charge density) in NIH-3T3 than that of LMSNCOOH-CUR@CS-FA indicated that the interaction of positively charged MSNs with the negatively charged cell membrane (adsorptive mediated endocytosis) can be the most probable mechanism of the cellular uptake. In addition, the antiproliferative effect of CUR with chitosan-folate coated was more sensitive for HeLa cells than NIH-3T3 cells (folate receptor negative).<sup>52</sup> Besides, the amphiphilic TPGS-PAE copolymer (D- $\alpha$ -tocopheryl polyethylene glycol 1,000-block-poly ( $\beta$ -amino ester)) as a pH-sensitive carrier was used to co-load Dox (a pro-apoptotic drug) and CUR (a potent drug for antiangiogenesis) by a one-step solvent evaporation method. The nanoparticles showed pH triggered obvious release behaviors in the endosomal environment of cancer cells. Over 90% of CUR were released at pH 5.8 after 192 hours, whereas 66.63% were released at pH 7.4. Its inhibition and apoptosis effect against SMMC 7721 cells were

enhanced in a synergistic manner through decreased mitochondrial membrane potential. The induced total apoptosis rates of free (Dox and CUR) and (Dox and CUR) NPs were 38.3% and 76.2%, respectively. In addition, these co-loaded NPs also showed stronger anti-angiogenic effects including inhibition of HUVEC proliferation, migration, invasion, and tube formation mediated VEGF pathway modulation.<sup>54</sup> It indicated that this co-delivery system of drugs with pro-apoptotic and anti-angiogenic activities is potentially effective in treating cancer.

The prodrug nano delivery system is also a good method for cancer treatment based on the weak acid environment of the tumor. In the study of Zhang et al,<sup>55</sup> the PEG-Dox nanoparticles (PEG-Dox NPs) were prepared through by Schiff's base reaction and self-assemble of Dox and PEG2000 in water at pH 7.4, and then encapsulate CUR into the core through hydrophobic interaction (PEG-Dox-CUR NPs). When PEG-Dox-CUR NPs were internalized into tumor cells, the Schiff's base linker between PEG2000 and Dox would be broken down in the acidic environment, leading to CUR release into the cytoplasm, which could avoid significant drug leakage in the blood circulation. As shown in Figure 5, after 24 hours, the Dox fluorescence intensities in the main organs were very weak, but were still strong in tumor tissues for PEG-Dox-CUR NP-treated mice. Furthermore, a better anti-tumor effect was observed on BALB/c nude mice

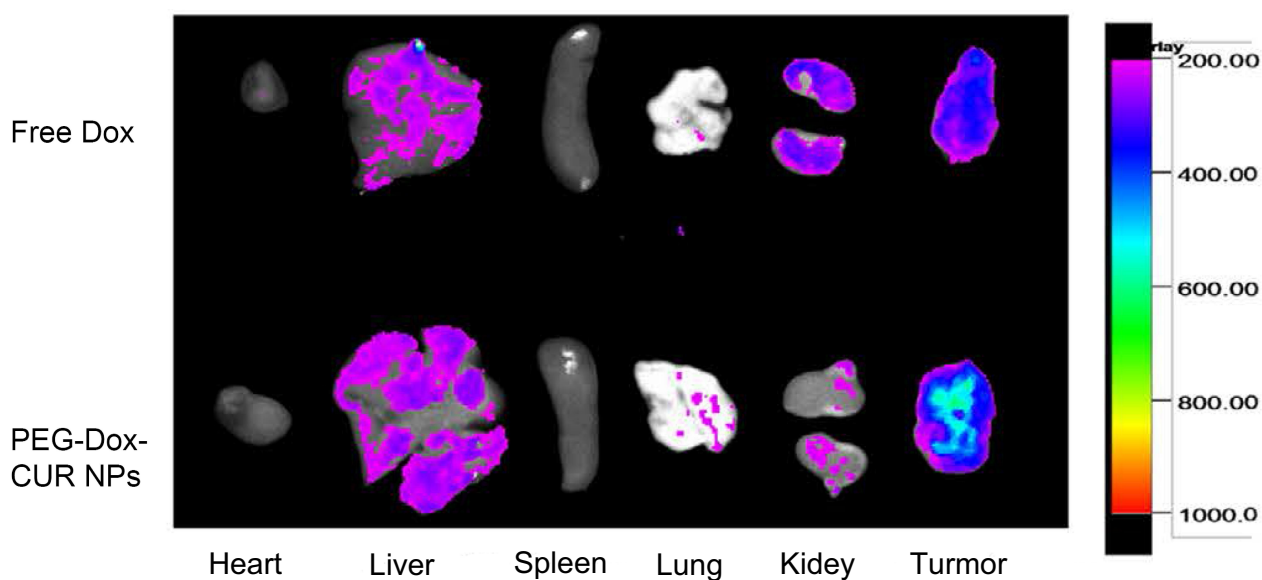


**Figure 5** Representative ex vivo images of tumor and main organs (heart, liver, spleen, lung, and kidney) after administration of DOX and PEG-Dox-CUR NPs. Reprinted from Zhang Y, Yang C, Wang W, et al. Co-delivery of doxorubicin and curcumin by pH-sensitive prodrug nanoparticle for combination therapy of cancer. *Sci Rep.* 2016;6(1):21225. This work is licensed under a Creative Commons Attribution 4.0 International License (<http://creativecommons.org/licenses/by/4.0/>).<sup>55</sup>

bearing HepG2 xenografts, the relative tumor volume of PBS, free Dox/CUR mixtures and PEG-Dox-CUR NPs was 1,000%, 500%, and 300%, respectively. However, some researchers have found that PEGylated nanoparticles are known to provoke certain immune responses after repeated dosing. When the PEGylated nanoparticles were repeatedly injected into the same animal (at intervals of several days), the long-term circulation characteristics were lost and the aggregation of PEG nanoparticles in the liver and spleen increased. Such immunogenicity of PEGylated nanoparticles present a barrier in the research of formulations and their use in the clinics.<sup>56,57</sup> Based on the Schiff base linkage of Dox and oxidized sodium alginate (Dox-OSA), the novel co-delivery (CUR and Dox) pH-sensitive nanoparticles were prepared by the self-assembly of amphiphilic macromolecular Dox-prodrug. When the feeding ratio of CUR/Dox/OSA was 1.4/4/10 (w/w/w), these nanoparticles showed higher drug encapsulation efficiency (Dox, 80.45%; CUR, 44.6%) and the drug loading capacity (Dox, 20.14%; CUR, 4.2%). The nanoparticles could selectively release drug into tumor cells due to the Schiff base linkage and showed a remarkable cytotoxicity in MCF-7 cells.<sup>58</sup> The prodrug delivery system with hydrophobic anticancer drugs deserves more extensive research. Besides, metal ion-CUR complexes could be a promising method to enhance the aqueous solubility of the hydrophobic drug and improve the anti-tumor effect. The Zn(II)-CUR nanoparticles (Zn(II)-CUR NPs) were prepared by solvent evaporation. The acid-labile coordination Zn(II)-O bond in Zn(II)-CUR NPs are broken, inducing the release of CUR responding to the tumor intracellular acidic environments. At pH 5, CUR was released about 90%, while only about 18% was released at pH 7.4 within 12 hours. Zn(II)-CUR NPs could effectively suppress the proliferation and migration growth on human bladder cancer cell lines HBC. As compared to the PBS control, the decreased tumor cell proliferation was observed for the Zn(II)-CUR NPs (79.54±5.09%).<sup>59</sup>

## CUR pH-Sensitive Micelles

Some representative pH sensitive chemical groups include polyacrylic acid, polymethacrylic acid, polyethyl acrylic acid, and other polybasic acids; sulfonamide group; polyamine, polyethyleneimine, and other basic groups; acid sensitive connection arm such as imine bond, hydrazide bond, hydrazone bond, cis-aconitamide, two methyl malimide, ether bond, ortho ester, and polyacetal (ketone).<sup>60</sup>

Based on the pH-sensitivity of these groups, many micelles were developed for drug controlled and specific release to achieve targeted therapy for lesions. The drug controlled release profile was mainly induced by protonated/deprotonated process and pH-sensitive bond breaking. Among that, the design ways of pH-sensitive CUR-loaded micelles for controlled release mainly include pH-sensitive carriers and prodrugs.

Based on the protonated/deprotonated process, many pH-sensitive CUR-loaded micelles consisting of pH sensitive materials were developed for targeted therapy. The amphiphilic BSCS was selected to encapsulate CUR for oral CUR delivery. Its carbonyl groups (succinic acids) could be protonated at acidic pH (1.2), resulting in limited release, but be ionized at basic pH (5.5, 6.8, and 7.4) leading to dissociation of micelles. At pH 1.2 (gastric fluid), about 30% of CUR was released from the micelles after 24 hours, whereas at pH 5.5, 6.8, and 7.4, about 70% of CUR was released. The IC<sub>50</sub> was 4.7-, 3.6-, and 12.2-fold lower than free CUR in HeLa, SiHa, and C33a cervical cell lines, respectively, and an increased early apoptosis (30–55%) was observed.<sup>61</sup> Hence the BSCS micelles can be used for effective intestinal delivery of CUR. A new pH-sensitive tri-block copolymer of PCL-PDEA-PSBMA was used for the CUR-loaded micelles. At pH 5.0 and pH 7.4, CUR was released about 73.3% and 52.4% after 12 hours, and the cumulative amount reached about 91.6% and 67.4% after 60 hours, respectively. It is because the PDEA block could be protonation leading to faster drug release in an acidic environment. The MRT<sub>(0-∞)</sub> (the mean retention time) and CL/z (the clearance) of CUR solution and CUR-loaded micelles was 62.365 h and 87.199 h, 0.298 and 0.223 L/h/kg, respectively. CUR-loaded micelles provided a higher clearance half-life (T<sub>1/2a</sub>) (8.52-fold), distribution half-life (T<sub>1/2b</sub>) (4.39-fold), AUC<sub>(0-∞)</sub> (1.34-fold), and MRT<sub>(0-∞)</sub> (1.40-fold) compared to the CUR solution.<sup>62</sup> It indicated that the tri-block copolymer of PCL-PDEA-PSBMA material used for encapsulating CUR can contribute to pH-sensitive controlled release and long circulation in vivo. This drug delivery system can increase the stability of CUR and resist its rapid metabolism in vivo. Similarly, CUR-loaded micelles, composed of poly(3-caprolactone)-b-poly(N,N-diethylaminoethyl methacrylate)-r-poly(N-(3-sulfopropyl)-N-methacryloxyethyl-N,N-diethylammonium) etainecopolymers (4s-PCL-PDEASB), also decreased CL/z (0.583 L/h/kg) compared to CUR solution (1.208 L/h/kg) and improved CUR bioavailability in rats. The AUC<sub>(0-∞)</sub>, C<sub>max</sub>, and t<sub>1/2</sub> of the CUR-loaded micelles were increased by 2.07-fold, 3.14-fold, and 1.42-fold, respectively compared to CUR

solution.<sup>63</sup> An endosomal micellar delivery system (F-pHSM-L61/CUR/Dox) consisting of a folate targeting ligand, poloxamer 407 (F127), and the pH-sensitive copolymer of PHis-PLA-PEG-PLA-Phis was used for multidrug resistance (MDR) reversal. The pH-sensitive copolymer PHis-PLA-PEG-PLA-Phis, composed of poly(ethylene glycol) (PEG), poly(D,L-lactide-co-glycolide) (PLA) and poly(l-histidine) (PHis), could disrupt the micellar structure triggering the release of Pluronic L61 unimers and CUR to the cytosol to exert their synergistic MDR reversal effect. At acidic pH, the imidazole groups of PHis block began to protonate inducing micellar structure destabilization and accelerated drug release. The IC<sub>50</sub> of F-pHSM-L61/CUR/DOX formulations against MCF-7/ADR cells was less than 2-fold to F-pHSM-L61/DOX formulations and less than 4-fold to F-pHSM/CUR/DOX formulation after 24-hour incubations.<sup>64</sup> One of the reasons for inducing MDR is the overexpression of ATP-binding cassette transporters (eg, P-gp and MRPs), which increase the efflux of drugs from cancer cells.<sup>65,66</sup> CUR and Pluronic unimers are capable of reversing MDR of tumors by regulating its expression and function.<sup>67,68</sup> Mechanistically, CUR and the Pluronic L61 unimers co-formulated pH-sensitive micelles exhibited a synergistic MDR reversal effect by inhibiting the expression and function of P-gp.

Based on pH-sensitive bond breaking, some micelles were designed to specifically deliver CUR to the target site such as polymer–drug conjugates. It can be achieved by introducing acid cleavable linkage to drugs/carrier materials to form a microenvironment responsive vesicle. The covalent bonds of polymer–drug conjugates would be broken down in an acid environment, resulting in drugs releasing rapidly. In a study, CUR dextran conjugate was synthesized with 2 g dextran, 0.2 g CUR hemi-succinate, 0.09 g DCC (N,N<sup>1</sup>-dicyclohexylcarbodiimide), 0.05 g DMAP (4-dimethylaminopyridine), and 0.04 g TEA (triethylamine) in 20 mL DMSO. The succinic acid spacer of CUR-dextran conjugate could be degraded at acidic pH, which afforded the capability of self-triggered drug release only at the tumor site and limited release at physiological pH. The sustained release (30.2±5.5%) of CUR-dextran micelles was observed at pH 7.4 in 72 hours, whereas an accelerated release (97.4±3.6%) was achieved at pH 4.5. The micelles had better therapeutic efficacy evidenced from the viability of C6 glioma cells (less than 20%) compared to free CUR (60%) at 50 μM CUR concentrations.<sup>69</sup> Moreover, the F68-CUR conjugates by covalently conjugating CUR to the hydrophilic terminals of Poloxam 188 (F68) chains via cis-aconitic anhydride linkers

was used for a novel flexible acid-responsive micelle formulation. The covalent bonds would be broken down leading to the faster release of CUR in a mildly acidic environment (pH 6.4 and pH 5.0) compared to in physiological pH 7.4. After 96 hours, almost 60% of CUR was released at pH 6.4 and 5.0, whereas only 40% CUR was released at pH 7.4. The IC<sub>50</sub> values of free CUR and F68-cis-CUR micelles were 43.78 and 18.46 μM in A2780 cells after 24 hours and were 22.92 and 10.15 μM for 48 hours, respectively. For SMMC 7721 cells, the IC<sub>50</sub> values of free CUR and F68-Cis-CUR micelles were 28.2 and 16.35 μM for 24 hours and were 15.54 and 7.63 μM for 48 hours, respectively.<sup>70</sup> These results proved prodrug delivery nano-systems is an effective way to improve the anticancer action. However, it often suffers from the slow drug release followed by delaying onset of pharmacological action. For example, the ester-linked conjugate micelles of mPEG-PLA-CUR, conjugated CUR to poly(lactic acid) (PLA) viagularic anhydride), showed slower drug release. After 24 hours, the amount released was only about 22% at pH 5.0. The IC<sub>50</sub> of the micelles and free CUR were 68.8 and 29 μM against HepG2 cells after 24 hours, respectively.<sup>71</sup> Fortunately, through the hydrazone linked CUR with mPEG-PLA, the hydrazone-linked polymer–CUR conjugate micelles (mPEG-PLA-Hyd-CUR) could increase the accumulated release, reaching about 55% at pH 5.0, attributing to the breaking down of hydrazone bonds. And it showed a better inhibitory effect on HepG2 cells (IC<sub>50</sub>, 27.7±5.3 μM after 24 hours).<sup>71</sup> In another study, mPEG-PLA was conjugated with CUR via tris(hydroxymethyl) aminomethane (Tris) linker to produce mPEG-PLA-Tris-CUR micelles by self-assembly. The drug loading capacity (18.5%, w/w)) has been greatly improved by the style of conjugations and drug encapsulation. The sustained release action was observed due to diffusion and hydrolysis of ester bonds. The accumulated release of pure CUR and the micelles was about 6% and 8%.<sup>72</sup> In addition, the material of mPEG-Chitosan-Ketal (PCK) was used to encapsulate CUR for pH-sensitive CUR-loaded ketal-based chitosan micelles, which could be selectively degraded in the acidic environment of the tumor. The tumor volume of free saline and CUR-loaded micelles was about 1,300 and 600 mm<sup>3</sup>, respectively. This suggested that the micelles could efficiently suppress tumor growth in vivo.<sup>73</sup>

## Other pH-Sensitive Preparation

There are some other kinds of pH-sensitive preparations, such as microspheres, molecular complexes, microcapsules. For example, pH triggered Eudragit-coated chitosan

microspheres of CUR for treating ulcerative colitis were initially prepared by emulsion cross-linking method and then coated with Eudragit® S100 that could prevent premature release of CUR in the upper gastrointestinal tract (GIT). An *in vivo* organ biodistribution study showed a negligible amount of CUR in the stomach ( $1.12 \pm 0.64\%$ ) and small intestine ( $2.63 \pm 0.87\%$ ), but high concentrations ( $51.23 \pm 2.53\%$ ) in the colon after 12 hours. Furthermore, the microspheres were evaluated by acetic acid-induced ulcerative colitis in mice. The CUR-loaded microspheres treated group exhibited mild lesions and inflammation, while the free CUR treated group showed moderate lesions and inflammatory reactions (Figure 6).<sup>74</sup> A study developed a molecular complexation of CUR with a pH-sensitive cationic copolymer of Eudragit® EPO by hydrogen bond formation and hydrophobic interactions using a nano precipitation method. It enhanced the aqueous solubility ( $>2$  mg/mL), increased peak plasma concentration (6 times) and improved bioavailability (about 20 times). The complexes were amorphous in solid and soluble only in buffers with pH less than 5.0.<sup>75</sup> Microcapsules containing CUR were prepared with poly(L-lysine), trisodium citrate and silica sol by self-assembly, which were also proved pH-sensitive drug release. The release of CUR was more triggered in an acidic environment than the basic (63% over acidic environment, pH 8.0) and neutral (35% over acidic environment, pH 7.0) condition. The more release of CUR would attribute to weakening of ionic interactions between the silica nanoparticles and poly(L-lysine) because of silica

particles losing its negative charges in an acidic environment.<sup>76</sup>

## Magnetic-Response Preparation

The basic principle of magnetic targeted drugs delivery system is that, in a magnetic field with a certain field strength, the magnetic carrier is gradually moved to the pathological area due to the flow properties and magnetic field induction properties of magnetic nanoparticles. Magnetic-response preparations are fabricated by three parts of magnetic core, skeleton material, and drug. Magnetic cores are usually prepared with Fe, Co, Ni, and ferrite materials ( $\text{Fe}_2\text{O}_3$ ,  $\text{Fe}_3\text{O}_4$ , ferromanganese oxygen, zinc ferrite) by co-precipitation method, microemulsion method, sol-gel method, hydrothermal synthesis method, and polyol process method.<sup>77,78</sup> The main magnetic core materials of ferrite are used for CUR-loaded magnetic-response preparations. At present, kinds of magnetic-response preparations of CUR are reported including magnetic nanoparticles, magnetic liposomes, magnetic hydrogel, magnetic microspheres, and nanospheres, etc.

## Magnetic Nanoparticles

Magnetic nanoparticles had excellent performances, such as biocompatibility, large specific surface area, low toxicity, high saturation magnetization, and magnetism.<sup>79,80</sup> They have been applied for magnetic resonance imaging,<sup>81</sup> catalysts, magnetic recording materials, and biomedicine,<sup>82</sup> especially anti-tumor therapy (eg, hepatoma cells and A549 cells).<sup>83–85</sup> When CUR combined with magnetic nanoparticles (CUR-MNPs), the



**Figure 6** Evaluation of experimental colitis in the colon of mice in (A) control group (severe lesions and inflammation), (B) CUR-treated group (moderate lesions), and (C) CUR microsphere-treated group (mild lesions). Reprinted with permission from Sareen R, Jain N, Rajkumari A, et al. pH triggered delivery of curcumin from Eudragit-coated chitosan microspheres for inflammatory bowel disease: characterization and pharmacodynamic evaluation. *Drug Delivery*. 2016;23(1):55–62. Copyright (2016) Taylor & Francis Ltd (<http://www.tandfonline.com>).<sup>74</sup>

antitumor effect can be enhanced due to the increasing drug concentrations in target tissues by magnetic targeting and drug controlled/sustained release. In addition, CUR-MNPs were also served as magnetic resonance imaging (MRI) contrast agents to diagnose and to improve targeting ability.

Cancer is the second leading cause of human deaths and was responsible for nearly one in six deaths worldwide.<sup>86</sup> Numerous chemotherapeutic drugs, even new drugs such as angiogenesis-targeted drugs and epidermal growth factor receptor-targeted drugs have been developed and used for the treatment of cancer.<sup>87–90</sup> However, the curative effects and application are not very good due to low 5-year survival rate, drug induced-toxicities, and resistance, etc.<sup>10,91,92</sup> There has been much interest in using magnetic targeted drug delivery system to treat tumors because of its unique physicochemical properties and good biocompatibility.<sup>79</sup> Magnetic mediated CUR-MNPs could concentrate CUR on desired cells or organs by an external magnetic field. In a study, DXS/PLL was synthesized with positive polyelectrolyte poly-L-lysine (PLL) and negative polyelectrolyte (DXS) by alternating incubations and used as nanocarriers for layer-by-layer polymer-coated magnetic nanoparticles. (DXS/PLL)-coated iron oxide MNPs showed a better uptake profile of CUR in SKOV-3 cells in an extracorporeal

magnetic field, as shown in Figure 7.<sup>93</sup> CUR-loaded superparamagnetic porous silica nanoparticles were developed for site-specific delivery of CUR under an external magnetic field. High loading of  $\text{Fe}_3\text{O}_4$  nanoparticles (37% wt) and CUR (30% wt) were incorporated into the porous silica matrix under mild conditions at room temperature. Briefly, a mixture of  $\text{H}_2\text{O}/\text{CTABr}/\text{HCl}/\text{formamide}$  was stirred at room temperature for 2 days, after which CUR (10 mg) and  $\text{Fe}_3\text{O}_4$  (100 mg) nanoparticles were added. After a day, tetraethylorthosilicate was added. The solution was then kept under quiescent conditions for 3 days. The molar ratio of  $\text{H}_2\text{O}/\text{HCl}/\text{formamide}/\text{CTABr}/\text{tetraethylorthosilicate}$  was 100:7.8:10.2:0.11:0.13.<sup>94</sup> This new synthetic methodology for preparing composite materials is likely to be applicable to other biologically active materials. A study prepared CUR-loaded magnetic nanoparticles with 810/300 mg  $\text{Fe}^{3+}/\text{Fe}^{2+}$  salts, 200 mg cyclodextrin (CD), and 250 mg F127, which could be efficiently internalized into human pancreatic cancer cells and improve mice survival. The amount of nanoparticle uptake was 54.06% for HPAF-II and 53.86% for Panc-1. The median survival was 40 days for MNPs and 24 days for Tween 20.<sup>34</sup> CUR has poor absorption and stability, which is the leading reason for its rapid metabolism and low oral bioavailability.<sup>14</sup> The

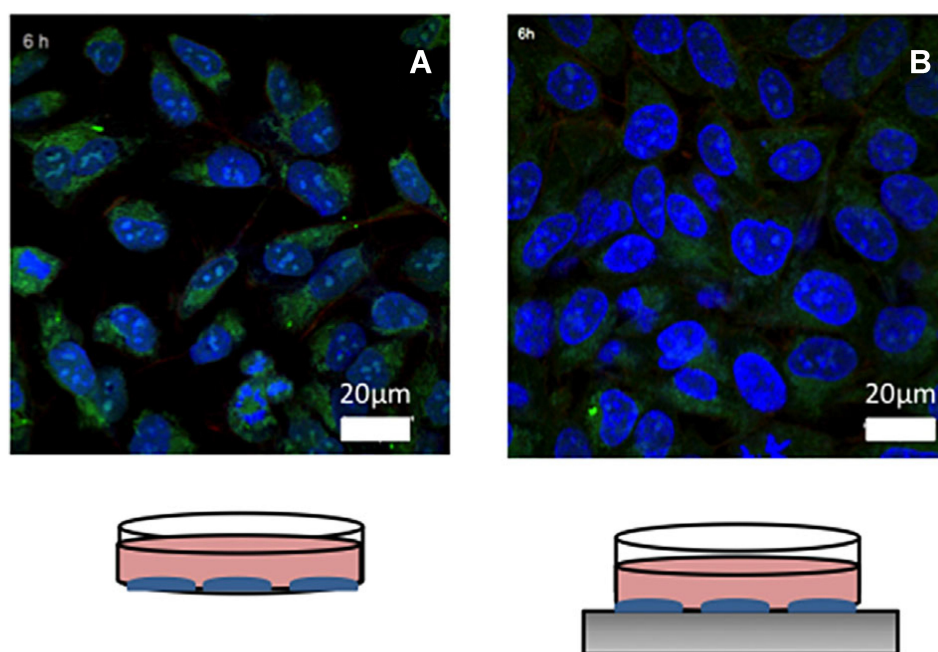


**Figure 7** Representative confocal images of (A) nano- $\text{Fe}_3\text{O}_4$ -coated with CUR on SKOV-3, and (B) nano- $\text{Fe}_3\text{O}_4$ -coated with CUR on SKOV-3 enhanced by magnetic field (Blue cells nuclei are labeled with DAPI, green nano- $\text{Fe}_3\text{O}_4$  are labeled with FITC (DXS-FITC), and red actin filaments are labeled with phalloidin-TRITC).

**Notes:** Reprinted with permission from Mancarella S, Greco V, Baldassarre F, et al. Polymer-coated magnetic nanoparticles for curcumin delivery to cancer cells. *Macromol Biosci*. 2015;15(10):1365–1374. © 2015 WILEY-VCH Verlag GmbH & Co. KGaA, Weinheim.<sup>93</sup>

**Abbreviations:** CUR, Curcumin; DAPI, 4',6-diamidino-2-phenylindole FITC (DXS-FITC), Fluorescein isothiocyanate-dextran.

CUR-loaded magnetic nanoparticles could improve the effective time and serum bioavailability of CUR in mice up to 2.5-fold through delayed-metabolism and increased accumulation in vivo. In addition, a considerable amount of CUR in MNP-CUR ( $1,792.19 \pm 644$  ng/mL) was observed at 6 hours, while only  $766.54 \pm 256$  ng/mL of CUR in Tween 20 was present.<sup>34</sup> This indicated that the stability of CUR was improved. CUR-MNPs can be used to enhance the therapeutic effect of CUR by increasing drug concentration and/or action time. In a study, CUR-loaded magnetic nanoparticles were prepared with epichlorohydrin- $\beta$ -cyclodextrin copolymer (Ep $\beta$ -CD) and oeoylextran. When the formulation of CUR-loaded magnetic nanoparticles contained 2/1 proportion of Ep $\beta$ -CD and oleoyldextran, it exhibited an improved drug release profile in extended manner up to 4 days (57.38%). In addition, the magnetization value of CUR-loaded magnetic nanoparticles was 58.23 emu/g, indicating paramagnetic behavior.<sup>95</sup> Therefore, CUR-loaded MNPs should be used for cancer therapy with some properties in the future.

MRI is produced by the radiation from the body material to the surrounding environment for helping disease diagnosis in the high frequency magnetic field. The two typical nanoparticles of quantum dots and magnetic nanoparticles have played important roles in the bioimaging field. Among them, magnetic nanoparticles serve as MRI contrast agents to improve the diagnostic sensitivity and specificity of MRI.<sup>96</sup> As mentioned previously, CUR has been used for anti-Alzheimer's disease. When combined with magnetic nanoparticles, it was used for visualized amyloid plaques diagnosis of Alzheimer's disease by MRI. The CUR-MNPs were not cytotoxic to either Madin-Darby canine kidney (MDCK) or differentiated human neuroblastoma cells (SH-SY5Y) and demonstrated amyloid plaque detection ability on AD Tg2576 mice brain sections. CUR-MNPs were prepared by a multi-inlet vortex mixer (MIVM). A superparamagnetic iron oxide core was firstly coated by a layer of CUR through hydrogen-bonding and then was encapsulated by polyethylene glycol-poly(lactic acid) (PEG-PLA) co-block polymer and polyvinylpyrrolidone (PVP) by a multi-inlet vortex mixer (MIVM).<sup>97,98</sup> CUR, used as an anti-oxidant, has been shown to reduce ROS damage for tissues and organs. Due to the presence of under-coordinated Fe atoms ( $\gamma$ -Fe<sub>2</sub>O<sub>3</sub>), surface-active maghemite nanoparticles (SAMNs) were modified with CUR on the nanoparticle surface, which had good properties as a MRI contrast agent and preserved the redox properties of CUR.<sup>99</sup> This CUR-modified SAMNs had a small size of  $13 \pm 4$  nm. Mouse fibroblasts test demonstrated that CUR-modified

SAMNs were well-tolerated on mammalian cells. Compared with uncoated SAMNs, the CUR-modified SAMNs core-shell composite was able to yield nearly comparable relaxivity indexes, with a longitudinal relaxation rate ( $r_1$ ) of  $0.266$  mM<sup>-1</sup> (Fe) s<sup>-1</sup> and transverse relaxation rate ( $r_2$ ) of  $28.05$  mM<sup>-1</sup> (Fe) s<sup>-1</sup>. The uncoated SAMNs system exhibited  $r_1$  of  $0.419$  mM<sup>-1</sup> (Fe) s<sup>-1</sup> and  $r_2$  of  $44.79$  mM<sup>-1</sup> (Fe) s<sup>-1</sup> at 293 K. The calculated  $r_2$  value rendered CUR-modified SAMNs an effective contrast agent material in MRI imaging (negative contrast). Besides, CUR-MNPs exhibited superior magnetic resonance imaging characteristics and significant tumor targeting capability. Yallapu et al<sup>100</sup> developed a composite MNP formulation composed of an iron oxide nanoparticle core coated with CD ( $\beta$ -cyclodextrin) and pluronic polymer (F68). The prepared CUR-MNPs had an individual particle grain size of  $<9$  nm and hydrodynamic average aggregative particle size of  $<123$  nm. The  $r_2$  order detected was  $7.040$  s<sup>-1</sup>  $\mu$ g<sup>-1</sup> mL (CUR-MNPs)  $> 4.38$  s<sup>-1</sup>  $\mu$ g<sup>-1</sup> mL (CUR-MNPs in cancer cells)  $> 3.40$  s<sup>-1</sup>  $\mu$ g<sup>-1</sup> mL (MNP)  $> 2.38$  s<sup>-1</sup>  $\mu$ g<sup>-1</sup> mL (MNP in cancer cells). The higher relaxivity values of CUR-MNPs were attributed to CUR and the nanoparticles induced greater inhomogeneity in the magnetic field than MNP. Moreover, CUR-MNPs were taken up in MDA-MB-231 cells through endocytosis. It displayed an antiproliferative effect with IC<sub>50</sub> of  $12.4$   $\mu$ M (free CUR,  $17.2$   $\mu$ M). This concluded that combined CUR and MNPs with ultra-low particle size, high inherent magnetic properties, effective imaging and targeting ability can be extended to preclinical and clinical applications for cancer treatment and imaging in the future.

## Functional Molecular Modified Magnetic Particles

In addition to described above about magnetic nanoparticles for targeted delivery, the drug is slowly selectively localized and released in a controlled manner (induced by targeting ligand/receptor or changes of physiological conditions such as pH), focusing on the target area to play a role. When CUR-loaded magnetic nanoparticles combined with ligand/receptor served as novel platforms for multiple biomedical applications, it could enhance the targeting and cellular uptake ability leading to an improved anticancer effect. For example, magnetite nanoaggregates were coated with poly(propylene glycol) bis(2-aminopropyl ether) (PPG-NH<sub>2</sub>) on its surface and then used to couple FA which served as a targeting ligand suggesting selective delivery towards MDA-MB-468 cells.

The CUR-loaded folic acid-conjugated magnetic nanoaggregates exhibited 3.9-fold higher level of cellular uptake than non-FA magnetic nanoaggregates.<sup>101</sup> In another study, magnetic nanoparticles were also modified with FA to obtain target specificity. N-[3(trimethoxysilyl) propyl]ethylenediamine was used to modify the MNPs to form a self-assembled monolayer and subsequently conjugated with folic acid and carboxymethylcyclodextrin through amidation between carboxy groups of folic acid/carboxymethylcyclodextrin and amine groups on the nanoparticle surface. Compared to non-folic acid magnetic targeted nanoparticles (23.4%), an enhanced cellular uptake was observed against C6 glioma cells (95.3%) by folic acid receptor mediated co-administration of paclitaxel and CUR.<sup>102</sup> When the physiological conditions (pH) changed, CUR was selectively released at the target area that could improve target ability and enhance the anti-tumor effect. For example, multi-layer iron oxide magnetic nanoparticles (Fe@HAP-PEI-CD or Fe@HAP-CD), consisting of hydroxyapatite (HAP),  $\beta$ -CD, and/or polyethyleneimine (PEI), also showed pH-sensitive drug release. Firstly, superparamagnetic iron oxide nanoparticles as a magnetically responsive core were prepared by a coprecipitation method, then grafted with PEI as a hydrophilic polymer to increase drug release at acidic pH, and lastly HAP and CD were used for coating and modifying to enhance the loading capacity. The significantly different release of Fe@HAP-PEI-CD (about 52%) and Fe@PEI-CD (38.1%) was obtained after 5 days at pH 5.5. However, a significant diminution was observed at pH 7.4 at the same times (Fe@HAP-PEI-CD, 28%; Fe@PEI-CD, 18.4%). The CUR-loaded multi-layer iron oxide magnetic nanoparticles were more effective than free CUR in suppressing MCF-7 breast cancer cells proliferation evidenced by the  $IC_{50}$  values of 40  $\mu$ M for free CUR, 22  $\mu$ M for Fe@PEI-CD, and 13  $\mu$ M for Fe@HAP-PEI-CD. In addition, the CLC and CLE for Fe@PEI-CD were 14.1% and 70.6%, respectively. Fe@HAP-PEI-CD showed more potential for CUR loading (CLC, 18% and CLE, 76.6%).<sup>103</sup> In another study, sulfobutyl ether- $\beta$ -CD and its derivatives functionalized MNPs (SBE- $\beta$ -CD-MNPs) were used to load CUR. The SBE- $\beta$ -CD-MNPs possessed excellent superparamagnetism with the remanence and coercivity of zero. The magnetization (58 emu/g) was enough for highly efficient magnetic manipulation when used as drug carriers in an external magnetic field. The loading efficiency of SBE- $\beta$ -CD-MNPs for CUR was high, up to 39.4%. The CUR-loaded SBE- $\beta$ -CD MNPs showed

favorable drug release property under the weak acid condition. About 76% of CUR were released at pH 5.3, but only 25% were released at pH 7.4 due to the hydrogen-bonding interaction between -OH groups of cyclodextrin ( $\beta$ -CD) and CUR. The CUR-loaded SBE- $\beta$ -CD MNPs showed an about 50% inhibition rate of HepG2 cells, but the SBE- $\beta$ -CD MNPs had no significant toxicity when concentrations were as high as 40  $\mu$ g/mL. Cell imaging demonstrated its successful internalization and distribution in the cell cytoplasm.<sup>104</sup> Besides, dual pH- and thermo-responsive magnetic preparations were reported for colon-specific drug delivery. When the pH was close to the neutral condition and the temperature raised to the body temperature, it could increase the cumulative release. CUR-loaded dual pH- and thermo-responsive magnetic microgels were prepared with pectin maleate, N-isopropyl acrylamide (10%) and  $Fe_3O_4$  nanoparticles (1%). In simulated intestinal fluid (SIF, pH 6.8) (25°C) the equilibrium was achieved after 35 hours (50%) without a magnetic field. However, the equilibrium was permitted at 80 hours (90%) under a magnetic field showing a slowly controlled and sustained CUR release. In simulated gastric fluid (SGF, pH 1.2) (25°C), the CUR release was not higher than 10% in the presence or absence of magnetic field. Moreover, in SGF (37°C), the released fraction of CUR was lower than 20%. However, in SIF (37°C), the amount of CUR released reached over 80% for all evaluated conditions. This enhanced release in SGF was mainly due to the galacturonic acid units over pectin being ionized, permitting repulsion among them, and hence the carrier was swelling, and diffusion to release drug in the colon site.<sup>105</sup>

## Magnetic Liposomes

Liposome is composed of amphiphilic molecules with a hydrophilic polar head and hydrophobic tail. CUR-loaded liposomes were used to treat many types of cancer, such as lung, cervical, prostate, breast, and liver cancer.<sup>10</sup> After loading magnetic nanoparticles, the liposomes have some magnetic-related characteristics such as heating generation and magnetic-targeted ability. It has been reported that temperatures in the range of 42–45°C are able to typically ablate cancer cells.<sup>106</sup> Therefore, the appropriate temperature is particularly important for the therapeutic effect. One study reported that CUR-loaded PEGylated magnetic liposomes exhibited rapid release at 45°C compared with 37°C, and the rapid release behavior was enhanced by magnetic heating under an

external high-frequency magnetic field (HFMF). Thus, the CUR-loaded PEGylated magnetic liposomes could increase the drug concentrations in the target site. The liposomes were prepared with 1,2-dipalmitoyl-sn-glycero-3-phosphocholine/cholesterol/1,2-distearoyl-sn-glycero-3-phosphoethanolamine N [carbonyl-methoxy(polyethylene glycol)-2000 lipid mixtures (80/20/5 mol%), oleic acid coated magnetic nanoparticles, and CUR in chloroform/methanol mixture (3/1, v/v) by a well-established thin-film hydration method (Figure 3). The CUR-loaded PEGylated magnetic liposomes could efficiently kill MCF-7 cells with  $IC_{50}$  of approximately 27.2  $\mu$ M for 48 hours. In addition, PEGylated magnetic liposomes showed no significant toxicity for 48 hours when the concentrations of PEGylated magnetic liposomes were as high as 1 mg/mL.<sup>107</sup> Therefore, the combination of magnetic targeting drug delivery systems and liposomes offer the potential application of CUR for cancer therapy through an inductive hyperthermia-triggering releasing system or magnetic heating therapy.

## Magnetic Microspheres and Nanospheres

Microspheres are a kind of particle dispersion system formed by drug dispersion or adsorption in the polymer or polymer matrix. The size range of microspheres is from 1–500  $\mu$ m, and microspheres with a size less than 500 nm are also called nanospheres. When combined with magnetic nanoparticles, microspheres have the properties of magnetic-response ability and magnetic fluid hyperthermia. A study developed CUR-loaded magnetic PLGA microspheres with a controllable particle size based on a composite emulsion. The microspheres containing hydrophilically modified  $Fe_3O_4$  nanoparticles, gelatin aqueous solution (0.5 wt %), PLGA (0.25 g), and PVA aqueous solution (poly(vinyl alcohol), 1 wt%) were prepared by water-in-oil-in-water method. Its mean particle size could be controlled by the manipulation of the osmotic pressure difference between the internal (gelatin) and external aqueous phases (PVA) via changing the glucose concentration. The mean particle size of the microspheres was 16–207  $\mu$ m with glucose concentrations from 0–20 wt %. It showed a rapid magnetic response, good superparamagnetism and a considerable magnetocaloric effect with a maximum magnetic entropy of 0.061 J/kg/K at 325 K. The magnetic microspheres also possessed good magnetic mobility, while the relatively low saturation

magnetization (5.293 emu/g) was observed.<sup>108</sup> Another study reported a poly(D,L-lactide-co-glycolide) (PLGA)-based controlled polymeric drug delivery system consisting of CUR and magnetic nanoparticles (MNPs). The PLGA nanospheres were prepared by the solvent evaporation method with polyvinyl alcohol as an emulsifying agent and acetone as a solvent phase. With an increase in PVA concentration from 1% to 7%, the size of the PLGA nanospheres decreased. After encapsulating MNPs, the average size of PLGA nanosphere decreased from >150 nm to 75 nm, which might be due to the surface charge stabilization with zeta potential value of –24 mV. The CUR-MNPs were served as a hyperthermic agent to induce cell death against HeLa cancer cells (90% higher than the control group) through magneto calorific effect (11.7 kA/m).<sup>109</sup> Such alternative treatment is a thermal therapy combined nanotechnology and hyperthermia. Namely, the biocompatible magnetic nanoparticles were injected into the tumor producing an increase in heat with external alternating magnetic field, which resulted in tumor cell ablation.<sup>110</sup> This indicated that the magnetic nanospheres can be useful as an agent for dual therapy in cancer treatment.

## Magnetic Hydrogel

Functional hydrogel produced through the incorporation of magnetic nanoparticles are used in biomedical applications with the properties of biocompatibility and the response to an external field. Previously, the clinical application of Dox has been restricted by its specific toxicities to cardiac tissues.<sup>111</sup> It has been reported that CUR has the activity of antimyocardial injury and preservation of cardiac function.<sup>112</sup> After being loaded to the magnetic hydrogel composites, CUR was reported to play a role of cardioprotective effects against dox-induced cardiac toxicity. This magnetic hydrogel nanocomposite was synthesized by dissolving the hydrogel in NaOH solution in the presence of CUR and magnetic nanoparticles. The drug loading and entrapment efficiency for CUR were 21% and 91%, respectively. The prepared magnetic hydrogel nanocomposites were uniform spherical nanoparticles with a mean diameter of 18–23 nm. The expression of three heart failure markers (atrial natriuretic peptide, B type natriuretic peptide, and beta major histocompatibility complex) decreases with an increase in the concentration of CUR ( $P < 0.05$ ). This combination can be considered as a potent therapy for heart failure and hypertension and



be a potential candidate to limit and mop-up free radical-mediated organ injury in the future.<sup>113</sup>

## Thermo-Sensitive Preparation

Thermo-sensitive gel could transform from liquid to non-chemical cross-linked semisolid gel due to the thermo-sensitivity of materials to external temperature.<sup>114</sup> Manifold thermo-sensitive polymers (such as collagen, chitosan, matrix gel, agarose, pluronic, poly(N-isopropylacrylamide) and poly(ethylene glycol) block polymers) could be used as or modified to be thermo-sensitive hydrogels.<sup>36</sup> As shown in Table 2, some polymers have been applied for temperature-mediated 'on/off' drug delivery of CUR and sustained drug delivery. In addition, a combination of other preparation delivery system with gel is also developed, such as liposomal-based/micelle-based thermo-sensitive gel. By this way, the properties of CUR were improved, involving control release, enhanced targeting, and therapy effect.

## Polymer Gel

For local administration (such as transdermal and nasal agent), the better thermo-sensitive property is forming gel in the short time under body temperature to prevent the loss of liquid. The most common material of poloxamer 407 (F127) used for thermo-sensitive gel is liquid at room temperature and transforms semisolid gelatin in the skin or mucosa, which is a kind of tri-block copolymer composed of 70% poly(ethylene oxide) and 30% poly(propylene oxide). Thus, the lowest critical solution temperature (LCST) of the gel for local administration is preferably regulated to about 37°C. The CUR-loaded microemulsion thermo-sensitive hydrogel was prepared with Capryol 90, Transcutal HP, Solutol HS, and F127. When the ratio of F-127 solution (21%) to microemulsion concentrate is more than 2/1, the gelling temperature of the system is below 37°C. After gelling, the hydrogel could be gelation at 37°C within 1 minute to control release and prevent CUR loss, and the cumulative release of CUR in vitro was 93.76% in 24 hours.<sup>115</sup> Additionally, a CUR-loaded temperature sensitive hydrogel was developed as local administration of the nasal cavity to improve the bioavailability of CUR in the brain. The gelation temperature of CUR-loaded temperature sensitive hydrogel (20% F-127, 2% F68, 0.02% Benza Australian gum, 0.9% uranium chloride, and 0.5% CUR) was 32±0.5°C, which was close to the physiological temperature of the nasal cavity (32–35°C). After local administration, the drug targeting efficiency (DTE) of the hydrogel in the brain, cerebellum,

hippocampus, and foam was 1.82, 2.05, 2.07, and 1.51 times that of intravenous administration, respectively, indicating that in situ gel administration significantly enhanced the brain targeting of CUR.<sup>116</sup> Another material of poly (N-vinylcaprolactam) (PNVC) was usually used to prepare the thermo-sensitive hydrogel because of its interesting LCST (varying between 32°C and 33°C). Poly (N-vinylcaprolactam-co-hydroxyl ethyl methacrylate) was obtained through free radical emulsion polymerization using methylene bis acrylamide as a cross-linker with N-vinylcaprolactam (NVCL) and hydroxyethyl methacrylate (HEMA). At 25°C (below LCST), the release of CUR from gels increased (about 88%), but at 37°C (above LCST) the cumulative release decreased (about 70%).<sup>117</sup> Therefore, the topical administration of nanogels are potentially useful for targeted drug delivery.

CUR-loaded temperature sensitive hydrogels for injection were also developed. The CUR thermo-sensitive hydrogels (CTH) for injection were prepared with 2 mg CUR, 20 g F127, 4 g F68, 8 mL PEG400, and 12 mL 1,2-propanediol for treatment of solid tumors (HCA-F, high lymphatic metastasis cells of mouse ascites hepatocellular carcinoma). It could prolong the retention time of 43.02 hours compared to CUR suspension for injection (10.89 hours).<sup>118</sup> Furthermore, the effectively inhibition of HCA-F cells was observed in vitro. After 24, 48, and 72 hours, the IC<sub>50</sub> was 2,430.6, 283.4, and 56.8 μM in the positive control group (fluorouracil injection), 685.8, 61.9, and 11.4 μM in the CTH group, and 1,017.1, 227.8, and 63.9 μM in the CUR suspension group, respectively.<sup>119</sup> For treatment of solid tumors, this intratumoral injection can increase the local drug concentration and retention through a thermo-sensitive drug delivery system.

## Liposomal-Based Thermo-Sensitive Gel

Liposomal-based thermo-sensitive gel is a pharmaceutical composite by combing of the liposome delivery system and thermo-gels technology. In this system, CUR is encapsulated with lipid carriers firstly and then dispersed in thermo-sensitive carriers. The liposomal-based thermo-sensitive gel had small size and high entrapment efficiency properties and effective anti-tumor and anti-inflammatory effects. In a study, CUR was loaded in nanostructured lipid carriers (CUR-NLCs) by the emulsion evaporation–solidification method at low temperature and was dispersed in F127 to form a thermo-sensitive in situ gel

(CUR-NLCs-Gel) for dermal delivery. CUR-NLCs and CUR-NLCs-Gel have similar results relating to parameters of uniform nano-sized spherical shape, mean size, entrapment efficiency, and drug loading of 263.9 nm, 91.76% and 2.19%, respectively. When the gels were applied to the skin topically, it could change from liquid to solid to decrease CUR loss and keep sustained skin drug delivery. The transdermal permeation rate of CUR could be significantly improved, and the cumulative amounts of CUR-NLCs, CUR-NLCs-Gel, and CUR propylene glycol solution were 2.453, 11.964, and 0.812  $\mu\text{g}\cdot\text{cm}^{-2}\cdot\text{h}^{-1}$ , respectively. Although the inhibition rates of CUR-NLCs-Gel (31.1%) were lower than indomethacin gel (65.7%) to auricle edemas induced by xylene in mice, CUR-NLCs-Gel showed a significant anti-inflammatory effect compared with the blank control group.<sup>120</sup> Another study reported a novel chitosan derivative for temperature and ultrasound dual-sensitive liposomal microbubble gel. Firstly, CUR was encapsulated with S100PC, N-cholesteryl hemisuccinate-O-sulfate chitosan, and cholesterol (90:3:10) to obtain a Cur-loaded liposome microbubble (CUR-LM) (Figure 3), and then was dispersed in chitosan/glycerol phosphate (CS/GP) solution to obtain a dual-sensitive liposomal microbubble gel (CUR-LM-G). The biocompatible chitosan/glycerol phosphate (CS/GP) gel as a carrier for liposomal microbubble was liquid at room temperature, but gels at 37°C under pH 7.4. The N-cholesteryl hemisuccinate-O-sulfate chitosan was carried to modified liposomal microbubble to enhance the property and blood-contacting stability of CUR. The mean particle size, mean zeta potential, and entrapment efficiency of Cur-LM was about 950 nm,  $-28.7\pm 3.8$  mV, and above 90%, respectively. The release of CUR was increased (85%), applying ultrasound on the CUR-LM-G compared with without applying ultrasound (32%). The tumor growth inhibition of Cur-LM-G in BALB/c mice with the ultrasound was higher than non-ultrasound evidenced by the tumor volume (about 480  $\text{mm}^3$  vs 600  $\text{mm}^3$ ), followed by the saline control group (about 1,200  $\text{mm}^3$ ).<sup>121</sup>

## Micelle-Based Thermo-Sensitive Gel

Micelles have been widely investigated with excellent properties such as improved therapeutic efficacy, solubility, selective targeting, reduced side-effects, and prolonged blood circulation for hydrophobic anticancer

drugs delivery.<sup>122–124</sup> Polymer micelles are core-shell structures formed by self-assembly of amphiphilic block copolymers, which could load different types of bioactive compounds inside the hydrophobic core. Micelle-based thermo-sensitive gels could retain the excellent properties of micelles and give them temperature response characteristics. After drug loading, the in vitro and in vivo properties of CUR were improved. These gels were mainly prepared by two types of dispersion and self-assembly method. One is to disperse CUR micelles in the thermo-sensitive hydrogel at sol state. For example, Zhang et al<sup>125</sup> prepared CUR-loaded polymeric micelles (CUR-M) by a solid dispersion method with monomethyl poly(ethylene glycol)-poly( $\epsilon$ -caprolactone) copolymer (MPEG-PCL) and mixing it with poly(ethylene glycol)-poly( $\epsilon$ -caprolactone)-poly(ethylene glycol) copolymer to obtain thermo-sensitive hydrogel (CUR-H) to treat colorectal cancer. The drug loading, encapsulation efficiency, and particle size of CUR-M were  $14.82\pm 0.07\%$ ,  $98.83\pm 0.45\%$ , and  $27.1\pm 1.3$  nm with a polydisperse index of  $0.149\pm 0.017$ , respectively. The CUR-H serving as a drug depot was a sol at ambient temperature and converted into gel at body temperature. CUR concentrations of the free CUR group in the abdominal cavity were much lower than those in the CUR-H group. The  $\text{AUC}_{0-24}$  and  $T_{1/2}$  values (2968.33  $\mu\text{g}\cdot\text{h}/\text{mL}$  and 3.692 h) of the CUR-H group in the abdominal cavity were 23.47-times and 6.51-times higher than those in the free CUR group. At day 22, the number and weight of tumor nodules (CT26 cells) in the CUR-H group was  $49.0\pm 15.4$  and  $0.88\pm 0.30$  g, vs  $92.5\pm 20.7$  ( $P<0.01$ ) and  $1.57\pm 0.24$  g ( $P<0.01$ ) in the CUR-M group and  $136.8\pm 14.3$  ( $P<0.001$ ) and  $2.19\pm 0.27$  g ( $P<0.001$ ) in the free CUR group. Therefore, the CUR-H could improve bioavailability and therapeutic effects of CUR through increasing the concentration and prolonging residence time in the abdominal cavity. Another method is the self-assembly process to form gel by encapsulating CUR directly in thermo-sensitive materials. For example, amphiphilic triblock copolymers containing a poly(L-lactide) (PLLA) central block and two poly(N-isopropylacrylamide-co-N,N-dimethylacrylamide) (P(NIPAAm-co-DMAAm)) lateral blocks were used to load CUR by self-assembly utilizing solvent evaporation/film hydration method. High drug loading (up to 20%) with high loading efficiency ( $>94\%$ ) were observed, and the LCST of drug loaded micelles was from 37.5 to 38.0°C, with drug loading increasing from 6.0 to 20%. The size of micelles ranged from 47.5–88.2 nm, remaining stable over 1 month with a zeta potential

from  $-12.4$  to  $-18.7$  mV. The initial burst release is observed and followed by a slower release with a higher release rate at  $40^{\circ}\text{C}$  (above the LCST) than  $37^{\circ}\text{C}$  due to thermo-responsive release. In addition, MTT assay and cell morphology results showed that P(NIPAAm-co-DMAAm)-b-PLLA-b-P(NIPAAm-co-DMAAm) copolymers present excellent cytocompatibility.<sup>126</sup> In general, micelle-based thermo-sensitive gel could be used for biomedical applications with outstanding properties, such as thermo-sensitive and sustained release, nano-scale size, high drug loading, and stability and good biocompatibility.

## Conclusion

Some physicochemical targeting preparations for enhancing the pharmacokinetics and pharmacodynamics properties of CUR were summarized, such as pH-sensitive preparations, magnetic target preparations, and thermo-sensitive preparations. Due to the microenvironment of tumors, inflammation regions and gastrointestinal tract, pH-sensitive preparation could increase the accumulation of CUR in specific sites due to its property of pH-dependent drug release. Through this local controlled release of drugs, the stability of CUR could be improved leading to an enhanced therapy effect of CUR. By applying the external magnetic field, magnetic nanoparticles could deliver CUR to a specific site and increase the amount of the drug in the target area. The magnetic nanoparticles in magnetic hyperthermia for cancers treatment and served as MRI contrast agents used in diagnosis have also already been carried out based on the magnetocaloric effect. Thermo-sensitive preparation could respond to temperature variation to increase the concentration in the target area. It was an effective method to retain drugs by intratumoral injection. In addition, the combination of pH-, magnetic, temperature-response system and ligand could be a promising strategy in clinical practice to treat cancers.

## Acknowledgments

This study was supported by the basic research fund of the science and technology department of Sichuan province of China (No. 2020YJ0336, 2020YJ0373), the Joint Fund of Luzhou City and Southwest Medical University (No. 2017LZXNYD-T02, 2019LZXNYDZ07), the Science and Technology Fund of Luzhou science and technology and Human Resources Bureau (No. 2019-SYF-35), Science and Technology Innovation Team from Jiucheng Science and Technology Talent Cultivation Plan in Luzhou City (No. 2019-1), the Scientific Research Foundation of

the Education Department of Sichuan Province (No. 17ZA0439, 18ZB0646), the research grant from Traditional Chinese Medicine Administration in Sichuan Province (No. 2018QN069).

## Disclosure

The authors report no conflicts of interest in this work.

## References

- Di Maio M, Basch E, Bryce J, Perrone F. Patient-reported outcomes in the evaluation of toxicity of anticancer treatments. *Nat Rev Clin Oncol.* 2016;13(5):951–955. doi:10.1038/nrclinonc.2015.222
- Cinci L, Mannelli LD, Maidecchi A, et al. Effects of Hypericum perforatum extract on oxaliplatin-induced neurotoxicity: in vitro evaluations. *Z Naturforsch C.* 2017;72(5–6):219–226. doi:10.1515/znc-2016-0194
- Malekinejad H, Ahsan S, Delkoshkasmaie F, et al. Cardioprotective effect of royal jelly on paclitaxel-induced cardio-toxicity in rats. *Iran J Basic Med Sci.* 2016;19(2):221–227.
- Mullally WJ, O'Suilleabhain CB, Brady C, et al. Vinorelbine induced perforation of a metastatic gastric lesion. *Irish J Med Sci.* 2017;186(3):571–575. doi:10.1007/s11845-016-1536-1
- Ninan PJ, Prasath D, James M. Toxicity and tolerability of paclitaxel and carboplatin regime in patients with epithelial ovarian cancer at a tertiary care hospital. *SSRG Int J Med Sci.* 2018;5(1):2393–9117.
- Zhao SJ, Pi C, Ye Y, Zhao L, Wei YM. Recent advances of analogues of curcumin for treatment of cancer. *Eur J Med Chem.* 2019;180:524–535. doi:10.1016/j.ejmech.2019.07.034
- Gupta SC, Patchva S, Aggarwal BB. Therapeutic roles of Curcumin: lessons learned from clinical trials. *AAPS J.* 2013;15(1):195–218. doi:10.1208/s12248-012-9432-8
- Moghadamtousi SZ, Kadir HA, Hassandarvish P, et al. A review on antibacterial, antiviral, and antifungal activity of curcumin. *Biomed Res Int.* 2014;2014(1):186864.
- Marchiani A, Rozzo C, Fadda A, et al. Curcumin and curcumin-like molecules: from spice to drugs. *Curr Med Chem.* 2014;21(2):204–222. doi:10.2174/092986732102131206115810
- Shen L, Liu L, Ji HF. Regulatory effects of curcumin spice administration on gut microbiota and its pharmacological implications. *Food Nutr Res.* 2017;61(1):1361780. doi:10.1080/16546628.2017.1361780
- Feng T, Wei Y, Lee RJ, et al. Liposomal curcumin and its application in cancer. *Int J Nanomed.* 2017;12:6027–6044. doi:10.2147/IJN.S132434
- Ramasamy TS, Ayob AZ, Myint HHL, et al. Targeting colorectal cancer stem cells using curcumin and curcumin analogues: insights into the mechanism of the therapeutic efficacy. *Cancer Cell Int.* 2015;15(1):96. doi:10.1186/s12935-015-0241-x
- Vishvakarma NK. Novel antitumor mechanisms of curcumin: implication of altered tumor metabolism, reconstituted tumor microenvironment and augmented myelopoiesis. *Phytochem Rev.* 2014;13(3):717–724. doi:10.1007/s11101-014-9364-2
- Prasad S, Tyagi AK, Aggarwal BB. Recent developments in delivery, bioavailability, absorption and metabolism of curcumin: the golden pigment from golden spice. *Cancer Res Treat.* 2014;46(1):2–18. doi:10.4143/crt.2014.46.1.2
- Yallapu MM, Nagesh PKB, Jaggi M, Chauhan SC. Therapeutic applications of curcumin nanoformulations. *AAPS J.* 2015;17(6):1341–1356. doi:10.1208/s12248-015-9811-z

16. Maeda H, Nakamura H, Fang J. The EPR effect for macromolecular drug delivery to solid tumors: improvement of tumor uptake, lowering of systemic toxicity, and distinct tumor imaging in vivo. *Adv Drug Deliv Rev.* 2013;65(1):71–79. doi:10.1016/j.addr.2012.10.002
17. Bertrand N, Wu J, Xu XY, Kamaly N, Farokhzad OC. Cancer nanotechnology: the impact of passive and active targeting in the era of modern cancer biology. *Adv Drug Deliv Rev.* 2014;66(1):2–25. doi:10.1016/j.addr.2013.11.009
18. Gera M, Sharma N, Ghosh M, et al. Nanoformulations of curcumin: an emerging paradigm for improved remedial application. *Oncotarget.* 2017;8(39):66680–66698. doi:10.18632/oncotarget.19164
19. Naksuriya O, Okonogi S, Schiffelers RM, et al. Curcumin nanoformulations: a review of pharmaceutical properties and preclinical studies and clinical data related to cancer treatment. *Biomaterials.* 2014;35(10):3365–3383. doi:10.1016/j.biomaterials.2013.12.090
20. Tajbakhsh A, Hasanzadeh M, Rezaee M, et al. Therapeutic potential of novel formulated forms of curcumin in the treatment of breast cancer by the targeting of cellular and physiological dysregulated pathways. *J Cell Physiol.* 2017;233:3.
21. Wei D, Hui L. Research progress in new formulation of curcumin for anti-tumor. *Acad J Second Military Med Univ.* 2015;36(7):771–775.
22. Lee WH, Loo CY, Young PM, et al. Recent advances in curcumin nanoformulation for cancer therapy. *Expert Opin Drug Deliv.* 2014;11(8):1183–1201. doi:10.1517/17425247.2014.916686
23. Dagar P, Dahiya P, Bhambi M. Recent advances in curcumin nanoformulations. *Nano Sci Nano Technol an Indian J.* 2014;8(12):458–474.
24. Hashemi M, Ebrahimian M. Recent advances in nanoformulations for co-delivery of curcumin and chemotherapeutic drugs. *Int J Nanomed.* 2017;4(1):1–7.
25. Wang M, Thanou M. Targeting nanoparticles to cancer. *Pharmacol Res.* 2010;62(2):90–99. doi:10.1016/j.phrs.2010.03.005
26. Wang JJ, Huang SW. Research progress on novel carrier-modified methods and evaluation of active targeting antitumor preparation. *Chin Herb Med.* 2014;6(1):22–28. doi:10.1016/S1674-6384(14)60002-2
27. Sonekar S, Mishra M, Patel A, et al. Formulation and evaluation of folic acid conjugated gliadin nanoparticles of curcumin for targeting colon cancer cells. *J Appl Pharm Sci.* 2016;6(10):068–074. doi:10.7324/JAPS.2016.601009
28. Wen X, Cheng X, Hu D, et al. Combination of curcumin with an anti-transferrin receptor antibody suppressed the growth of malignant gliomas in vitro. *Turk Neurosurg.* 2016;26(2):209–214.
29. Mulik RS, Mönkkönen J, Juvonen RO, et al. Transferrin mediated solid lipid nanoparticles containing curcumin: enhanced in vitro anticancer activity by induction of apoptosis. *Int J Pharm.* 2010;398(1):190–203. doi:10.1016/j.ijpharm.2010.07.021
30. Felber AE, Dufresne MH, Leroux JC. pH-sensitive vesicles, polymeric micelles, and nanospheres prepared with polycarboxylates. *Adv Drug Deliv Rev.* 2012;64(11):979–992. doi:10.1016/j.addr.2011.09.006
31. Tila D, Yazdaniarazi SN, Ghanbarzadeh S, et al. pH-sensitive, polymer modified, plasma stable niosomes: promising carriers for anti-cancer drugs. *Excli Journal.* 2015;14(4):21.
32. Hu FQ, Zhang YY, You J, et al. pH triggered doxorubicin delivery of PEGylated glycolipid conjugate micelles for tumor targeting therapy. *Mol Pharm.* 2012;9(9):2469–2478. doi:10.1021/mp300002v
33. Wu T, Hua MY, Chen JP, et al. Effects of external magnetic field on biodistribution of nanoparticles: A histological study. *J Magn Magn Mater.* 2007;311(1):372–375. doi:10.1016/j.jmmm.2006.10.1202
34. Yallapu MM, Ebeling MC, Khan S, et al. Novel curcumin-loaded magnetic nanoparticles for pancreatic cancer treatment. *Mol Cancer Ther.* 2013;12(8):1471–1480. doi:10.1158/1535-7163.MCT-12-1227
35. Cui Y, Zhang M, Zeng F, Jin HY, Xu Q, Huang YZ. Dual-targeting magnetic PLGA nanoparticles for codelivery of paclitaxel and curcumin for brain tumor therapy. *ACS Appl Mater Inter.* 2016;8(47):32159–32169. doi:10.1021/acsami.6b10175
36. Li ZQ, Guan JJ. Thermosensitive hydrogels for drug delivery. *Expert Opin Drug Deliv.* 2011;8(8):991–1007. doi:10.1517/17425247.2011.581656
37. Vaupel P. Tumor microenvironmental physiology and its implications for radiation oncology. *Semin Radiat Oncol.* 2004;14(3):198–206. doi:10.1016/j.semradonc.2004.04.008
38. Bueno PVA, Souza PR, Follmann HDM, et al. N,N-Dimethyl chitosan/heparin polyelectrolyte complex vehicle for efficient heparin delivery. *Int J Biol Macromol.* 2015;75:186–191. doi:10.1016/j.ijbiomac.2015.01.030
39. Talaie F, Atyabi F, Azjdarzadeh M, et al. Overcoming therapeutic obstacles in inflammatory bowel diseases: A comprehensive review on novel drug delivery strategies. *Eur J Pharm Sci.* 2013;49(4):712–722. doi:10.1016/j.ejps.2013.04.031
40. Ju L, Cailin F, Wenlan W, et al. Preparation and properties evaluation of a novel pH-sensitive liposomes based on imidazole-modified cholesterol derivatives. *Int J Pharm.* 2016;518(1–2):213–219. doi:10.1016/j.ijpharm.2016.11.044
41. Moku G, Gulla SK, Nimmu NV, et al. Delivering anti-cancer drugs with endosomal pH-sensitive anti-cancer liposomes. *Biomater Sci.* 2016;4(4):627–638. doi:10.1039/C5BM00479A
42. Jelezova I, Drakalska E, Momekova D, et al. Curcumin loaded pH-sensitive hybrid lipid/block copolymer nanosized drug delivery systems. *Eur J Pharm Sci.* 2015;78:67–78. doi:10.1016/j.ejps.2015.07.005
43. De LV, Milano F, Mancini E, et al. Encapsulation of curcumin-loaded liposomes for colonic drug delivery in a pH-responsive polymer cluster using a pH-driven and organic solvent-free process. *Molecules.* 2018;23(4):739. doi:10.3390/molecules23040739
44. Gugulothu D, Kulkarni A, Patravale V, et al. pH-sensitive nanoparticles of curcumin–celecoxib combination: evaluating drug synergy in ulcerative colitis model. *J Pharm Sci.* 2014;103(2):687–696. doi:10.1002/jps.23828
45. Dandekar P, Dhupal R, Jain R, et al. Toxicological evaluation of pH-sensitive nanoparticles of curcumin: acute, sub-acute and genotoxicity studies. *Food Chem Toxicol.* 2010;48(8):2073–2089. doi:10.1016/j.fct.2010.05.008
46. Wahlstrom B, Blennow G. A study on the fate of curcumin in the rat. *Acta Pharmacol Toxicol.* 1978;43(2):86–92. doi:10.1111/j.1600-0773.1978.tb02240.x
47. Belouqui A, Coco R, Memvanga PB, et al. pH-sensitive nanoparticles for colonic delivery of curcumin in inflammatory bowel disease. *Int J Pharm.* 2014;473(1–2):203–212.
48. Prajakta D, Ratnesh J, Chandan K, et al. Curcumin loaded pH-sensitive nanoparticles for the treatment of colon cancer. *J Biomed Nanotechnol.* 2009;5(5):445–455. doi:10.1166/jbn.2009.1038
49. Huang YC, Lam UI. Chitosan/fucoidan pH sensitive nanoparticles for oral delivery system. *J Chin Chem Soc.* 2011;58(6):779–785. doi:10.1002/jccs.201190121
50. Abouaitah KE, Farghali AA, Swiderska-Sroda A, et al. pH-controlled release system for curcumin based on functionalized dendritic mesoporous silica nanoparticles. *J Nanomed Nanotechnol.* 2016;7(1):351.
51. Kim S, Philippot S, Fontanay S, et al. pH- and glutathione-responsive release of curcumin from mesoporous silica nanoparticles coated using tannic acid-Fe(III) complex. *RSC Adv.* 2015;5(110):90550–90558. doi:10.1039/C5RA16004A

52. Daryasari MP, Akhgar MR, Mamashli F, et al. Chitosan-folate coated mesoporous silica nanoparticles as a smart and pH-sensitive system for curcumin delivery. *RSC Adv.* 2016;6(107):105578–105588. doi:10.1039/C6RA23182A
53. Gao Y, Li Y, Li Y, et al. PSMA-mediated endosome escape-accelerating polymeric micelles for targeted therapy of prostate cancer and the real time tracing of their intracellular trafficking. *Nanoscale.* 2014;7(2):597–612. doi:10.1039/C4NR05738D
54. Zhang J, Li J, Shi Z, et al. pH-sensitive polymeric nanoparticles for co-delivery of doxorubicin and curcumin to treat cancer via enhanced pro-apoptotic and anti-angiogenic activities. *Acta Biomater.* 2017;58:349–364. doi:10.1016/j.actbio.2017.04.029
55. Zhang Y, Yang C, Wang W, et al. Co-delivery of doxorubicin and curcumin by pH-sensitive prodrug nanoparticle for combination therapy of cancer. *Sci Rep.* 2016;6(1):21225. doi:10.1038/srep21225
56. Lu W, Wan J, She ZJ, Jiang XG. Brain delivery property and accelerated blood clearance of cationic albumin conjugated pegylated nanoparticle. *J Control Release.* 2007;118(1):38–53. doi:10.1016/j.jconrel.2006.11.015
57. Ishihara T, Takeda M, Sakamoto H, et al. Accelerated blood clearance phenomenon upon repeated injection of PEG-modified PLA-nanoparticles. *Pharm Res.* 2009;26(10):2270–2279. doi:10.1007/s11095-009-9943-x
58. Gao C, Tang F, Gong G, et al. pH-Responsive prodrug nanoparticles based on a sodium alginate derivative for selective co-release of doxorubicin and curcumin into tumor cells. *Nanoscale.* 2017;9(34):12533. doi:10.1039/C7NR03611F
59. Xing ZH, Wei JH, Cheang TY, et al. Bifunctional pH-sensitive Zn(II)-curcumin nanoparticles/siRNA effectively inhibit growth of human bladder cancer cells. *J Mater Chem B.* 2014;2(18):2714–2724. doi:10.1039/c3tb21625j
60. Wang DS, Zhou YX, Li CW, et al. Recent progress in research of pH-sensitive polymeric micelles as drug delivery system. *Chin J New Drugs.* 2016;25(19):2218–2224.
61. Sajomsang W, Gonil P, Saesoo S, et al. Synthesis and anticervical cancer activity of novel pH responsive micelles for oral curcumin delivery. *Int J Pharm.* 2014;477(1–2):261–272. doi:10.1016/j.ijpharm.2014.10.042
62. Zhai S, Ma Y, Chen Y, et al. Synthesis of an amphiphilic block copolymer containing zwitterionic sulfobetaine as a novel pH-sensitive drug carrier. *Polym Chem.* 2014;5(4):1285–1297.
63. Wu Z, Cai M, Xie X, et al. The effect of architecture/composition on the pH sensitive micelle properties and in vivo study of curcumin-loaded micelles containing sulfobetaines. *RSC Adv.* 2015;5(129):106989–107000. doi:10.1039/C5RA20847E
64. Wei H, Shi H, Qiao M, et al. pH-sensitive micelles for the intracellular co-delivery of curcumin and Pluronic L61 unimers for synergistic reversal effect of multidrug resistance. *Sci Rep.* 2017;7:42465. doi:10.1038/srep42465
65. Plasschaert SLA, de Bont ESJM, Boezen M, et al. Expression of multidrug resistance-associated proteins predicts prognosis in childhood and adult acute lymphoblastic leukemia. *Clin Cancer Res.* 2005;11(24 Pt 1):8661–8668. doi:10.1158/1078-0432.CCR-05-1096
66. Szakacs G, Paterson JK, Ludwig JA, Booth-Genthe C, Gottesman MM. Targeting multidrug resistance in cancer. *Nat Rev Drug Discov.* 2006;5(3):219–234.
67. Alvarez AI, Real R, Pérez MG, Prieto JG, Merino G. Modulation of the activity of ABC transporters (P-glycoprotein, MRP2, BCRP) by flavonoids and drug response. *J Pharm Sci.* 2010;99(2):598–617. doi:10.1002/jps.21851
68. Evers R, Kool M, Smith AJ, van Deemter L, de Haas M, Borst P. Inhibitory effect of the reversal agents V-104, GF120918 and Pluronic L61 on MDR1 Pgp-, MRP1- and MRP2-mediated transport. *Br J Cancer.* 2000;83(3):366–374. doi:10.1054/bjoc.2000.1260
69. Raveendran R, Bhuvaneshwar GS, Sharma CP. Hemocompatible curcumin-dextran micelles as pH sensitive pro-drugs for enhanced therapeutic efficacy in cancer cells. *Carbohydr Polym.* 2016;137:497–507. doi:10.1016/j.carbpol.2015.11.017
70. Fang XB, Zhang JM, Xie X, et al. pH-sensitive micelles based on acid-labile pluronic F68-curcumin conjugates for improved tumor intracellular drug delivery. *Int J Pharm.* 2016;502(1–2):28–37. doi:10.1016/j.ijpharm.2016.01.029
71. Li H, Li M, Chen C, et al. On-demand combinational delivery of curcumin and doxorubicin via a pH-labile micellar nanocarrier. *Int J Pharm.* 2015;495(1):572–578. doi:10.1016/j.ijpharm.2015.09.022
72. Yang RL, Zhang SA, Kong DL, et al. Biodegradable polymer-curcumin conjugate micelles enhance the loading and delivery of low-potency curcumin. *Pharm Res.* 2012;29(12):3512–3525. doi:10.1007/s11095-012-0848-8
73. Yu H, Mu H, Xiu L, et al. A novel ketal-based chitosan as nano-vehicles for potential pH-sensitive nanomedicine delivery. *Nanosci Nanotech Lett.* 2013;5(9):1007–1011. doi:10.1166/nl.2013.1660
74. Sareen R, Jain N, Rajkumari A, et al. pH triggered delivery of curcumin from Eudragit-coated chitosan microspheres for inflammatory bowel disease: characterization and pharmacodynamic evaluation. *Drug Deliv.* 2016;23(1):55–62.
75. Kumar S, Kesharwani Himanshi Mathur SS, Tyagi M, et al. Molecular complexation of curcumin with pH sensitive cationic copolymer enhances the aqueous solubility, stability and bioavailability of curcumin. *Eur J Pharm Sci.* 2016;82:86–96. doi:10.1016/j.ejps.2015.11.010
76. Patra D, Sleem F. A new method for pH triggered curcumin release by applying poly(L-lysine) mediated nanoparticle-congregation. *Anal Chim Acta.* 2013;795(18):60–68. doi:10.1016/j.aca.2013.07.063
77. Lin YP, Zhang K, Zhang RH, et al. Magnetic nanoparticles applied in targeted therapy and magnetic resonance imaging: crucial preparation parameters, indispensable pre-treatments, updated research advancements and future perspectives. *J Mater Chem B.* 2020;8(28):5973–5991. doi:10.1039/D0TB00552E
78. Asnaashari Eivari H, Rahdar A, Arabi H. Preparation of super paramagnetic iron oxide nanoparticles and investigation their magnetic properties. *Int J Eng Sci Invest.* 2012;1(3):2251–8843.
79. Gao YL, Zhu GM, Ma TT. Progress in Fe<sub>3</sub>O<sub>4</sub> magnetic nanoparticles and its application in biomedical fields. *Chem Ind Eng Prog.* 2017;36(3):973–980.
80. Pankhurst QA, Connolly JS, Jones SK, Dobso J. Application of magnetic nanoparticles in biomedicine. *J Phys D Appl Phys.* 2003;36(13):R167–R181. doi:10.1088/0022-3727/36/13/201
81. Janjic JM, Shao P, Zhang S, et al. Perfluorocarbon nanoemulsions with fluorescent, colloidal and magnetic properties. *Biomaterials.* 2014;35(18):4958–4968. doi:10.1016/j.biomaterials.2014.03.006
82. Yan H, Zhang JC, You CX, Song ZW, Yu BW, Shen Y. Surface modification of Fe<sub>3</sub>O<sub>4</sub> nanoparticles and their magnetic properties. *Int J Min Met Mater.* 2009;16(002):226–229. doi:10.1016/S1674-4799(09)60038-8
83. Jain TK, Richey J, Strand M, Leslie-Pelecky DL, Flask CA, Labhasetwar V. Magnetic nanoparticles with dual functional properties: drug delivery and magnetic resonance imaging. *Biomaterials.* 2008;29(29):4012–4021. doi:10.1016/j.biomaterials.2008.07.004
84. Pilapong C, Sitthichai S, Thongtem S, Thongtem T. Smart magnetic nanoparticle-aptamer probe for targeted imaging and treatment of hepatocellular carcinoma. *Int J Pharm.* 2014;473(1–2):469–474. doi:10.1016/j.ijpharm.2014.07.036
85. Kasai H, Kawai K, Shiraishi T, et al. Effects of Fe<sub>3</sub>O<sub>4</sub> Magnetic Nanoparticles on A549 Cells. *Int J Mol Sci.* 2013;14(8):15546–15560. doi:10.3390/ijms140815546

86. Polo E, Pino PD, Pardo A, et al. Magnetic nanoparticles for cancer therapy and bioimaging. *Nanooncology*. 2018;239–279.
87. Sideris S, Aoun F, Zanaty M, et al. Efficacy of weekly paclitaxel treatment as a single agent chemotherapy following first-line cisplatin treatment in urothelial bladder cancer. *Mol Clin Oncol*. 2016;4(6):1063–1067. doi:10.3892/mco.2016.821
88. Bae YJ, Yoon YI, Yoon TJ, et al. Ultrasound-guided delivery of siRNA and a chemotherapeutic drug by using microbubble complexes: in vitro and in vivo evaluations in a prostate cancer model. *Korean J Radiol*. 2016;17(4):497–508.
89. Meador CB, Jin H, De SE, et al. Optimizing the sequence of anti-EGFR targeted therapy in EGFR-mutant lung cancer. *Mol Cancer Ther*. 2015;14(2):542–552. doi:10.1158/1535-7163.MCT-14-0723
90. Yonesaka K, Hirotsu K, Kawakami H, et al. Anti-HER3 monoclonal antibody patritumab sensitizes refractory non-small cell lung cancer to the epidermal growth factor receptor inhibitor erlotinib. *Oncogene*. 2015;35(7):878–886. doi:10.1038/onc.2015.142
91. Zhou Q, Ye M, Lu Y, et al. Curcumin improves the tumoricidal effect of mitomycin C by suppressing ABCG2 expression in stem cell-like breast cancer cells. *PLoS One*. 2015;10(8):e0136694. doi:10.1371/journal.pone.0136694
92. Talekar M, Ouyang Q, Goldberg MS, et al. Cosilencing of PKM-2 and MDR-1 sensitizes multidrug-resistant ovarian cancer cells to paclitaxel in a murine model of ovarian cancer. *Mol Cancer Ther*. 2015;14(7):1521–1531. doi:10.1158/1535-7163.MCT-15-0100
93. Mancarella S, Greco V, Baldassarre F, et al. Polymer-coated magnetic nanoparticles for curcumin delivery to cancer cells. *Macromol Biosci*. 2015;15(10):1365–1374. doi:10.1002/mabi.201500142
94. Chin SF, Iyer KS, Saunders M, et al. Encapsulation and sustained release of curcumin using superparamagnetic silica reservoirs. *Chem-Eur J*. 2010;15(23):5661–5665. doi:10.1002/chem.200802747
95. Silambarasi T, Latha S. Formulation and evaluation of curcumin loaded magnetic nanoparticles for cancer therapy. *Int J Pharm Sci & Res*. 2012;3(5):1–16.
96. Latorre M, Rinaldi C. Applications of magnetic nanoparticles in medicine: magnetic fluid hyperthermia. *P R Health Sci J*. 2009;28(3):227–238.
97. Cheng KK, Wang YX, Chow AHL, et al. Amyloid plaques binding curcumin conjugated magnetic nanoparticles for diagnosis in Alzheimer's disease TG2576 mice. *Alzheimers Dement*. 2014;10(4):152–153. doi:10.1016/j.jalz.2014.04.122
98. Cheng KK, Chan PS, Fan S, et al. Curcumin-conjugated magnetic nanoparticles for detecting amyloid plaques in Alzheimer's disease mice using magnetic resonance imaging (MRI). *Biomaterials*. 2015;44(44):155–172. doi:10.1016/j.biomaterials.2014.12.005
99. Magro M, Campos R, Baratella D, et al. A magnetically drivable nanovehicle for curcumin with antioxidant capacity and MRI relaxation properties. *Chemistry*. 2015;20(37):11913–11920. doi:10.1002/chem.201402820
100. Yallapu MM, Othman SF, Curtis ET, et al. Curcumin-loaded magnetic nanoparticles for breast cancer therapeutics and imaging applications. *Int J Nanomed*. 2012;7(1):1761–1779.
101. Salem M. Curcumin-loaded magnetic nanoaggregates conjugated with folic acid for targeted cancer treatment. *Electronic Thesis Dissertation Repository*. 2014;2206.
102. Manju S, Sharma CP, Sreenivasan K. Targeted coadministration of sparingly soluble paclitaxel and curcumin into cancer cells by surface engineered magnetic nanoparticles. *J Mater Chem*. 2011;21(39):15708–15717. doi:10.1039/c1jm12528a
103. Akrami M, Khoobi M, Khalilvand-Sedagheh M, et al. Evaluation of multilayer coated magnetic nanoparticles as biocompatible curcumin delivery platforms for breast cancer treatment. *RSC Adv*. 2015;5(107):88096–88107. doi:10.1039/C5RA13838H
104. Zhou Y, Wang C, Wang F, et al.  $\beta$ -Cyclodextrin and its derivatives functionalized magnetic nanoparticles for targeting delivery of curcumin and cell imaging. *Chin J Chem*. 2016;34(6):599–608. doi:10.1002/cjoc.201500756
105. Almeida EAMS, Belletini IC, Garcia FP, et al. Curcumin-loaded dual pH- and thermo-responsive magnetic microcarriers based on pectin maleate for drug delivery. *Carbohydr Polym*. 2017;171:259–266. doi:10.1016/j.carbpol.2017.05.034
106. Tang YD, Jin T, Flesch RCC. Numerical temperature analysis of magnetic hyperthermia considering nanoparticle clustering and blood vessels. *IEEE T Magn*. 2017;53(10):1–6. doi:10.1109/TMAG.2017.2722425
107. Hardiansyah A, Yang MC, Liu TY, et al. Hydrophobic drug-loaded PEGylated magnetic liposomes for drug-controlled release. *Nanoscale Res Lett*. 2017;12(1):355. doi:10.1186/s11671-017-2119-4
108. Hu L, Huang M, Wang J, et al. Preparation of magnetic poly (lactic-co-glycolic acid) microspheres with a controllable particle size based on a composite emulsion and their release properties for curcumin loading. *J Appl Polym Sci*. 2016;133(16):43317. doi:10.1002/app.43317
109. Kini S, Bahadur D, Panda D. Magnetic PLGA nanospheres: a dual therapy for cancer. *Ieee T Magn*. 2011;47(10):2882–2886. doi:10.1109/TMAG.2011.2158403
110. Hu RL, Ke XF, Jiang H, et al. Effect of interleukin-2 treatment combined with magnetic fluid hyperthermia on Lewis lung cancer-bearing mice. *Biomed Rep*. 2016;50(1):59–62. doi:10.3892/br.2015.540
111. Zhou S, Palmeira CM, Wallace KB. Doxorubicin-induced persistent oxidative stress to cardiac myocytes. *Toxicol Lett*. 2001;121(3):151–157. doi:10.1016/S0378-4274(01)00329-0
112. Srivastava G, Mehta JL. Currying the heart: curcumin and cardioprotection. *J Cardiovasc Pharmacol Ther*. 2009;14(1):22–27. doi:10.1177/1074248408329608
113. Namdari M, Eatemadi A. Cardioprotective effects of curcumin-loaded magnetic hydrogel nanocomposite (nanocurcumin) against doxorubicin-induced cardiac toxicity in rat cardiomyocyte cell lines. *Artif Cell Nanomed B*. 2017;45(4):731–739. doi:10.1080/21691401.2016.1261033
114. Rahman CV, Kuhn G, White LJ, et al. PLGA/PEG-hydrogel composite scaffolds with controllable mechanical properties. *J Biomed Mater Res B*. 2013;101B(4):648–655. doi:10.1002/jbm.b.32867
115. Li XY, Dou JF, Wang S, Zhang L, Zhai GX. Preparation and characteristics of curcumin loaded microemulsion based in situ thermosensitive gelling system. *Pharm Biotechnol*. 2013;020(003):225–228.
116. Chen X, Zhi F, Jia X, et al. Enhanced brain targeting of curcumin by intranasal administration of a thermosensitive poloxamer hydrogel. *J Pharm Pharmacol*. 2013;65(6):807–816. doi:10.1111/jphp.12043
117. Sudhakar K, Rao KM, Subha MCS, et al. Temperature-responsive poly-(vinylcaprolactam-co-hydroxyethyl methacrylate) nanogels for controlled release studies of curcumin. *Des Monomers Polym*. 2015;18(8):705–713. doi:10.1080/15685551.2015.1070497
118. Gao M, Bao X, Lei AN, et al. Retention time of curcumin thermosensitive hydrogels for injection in solid tumor. *China Pharm*. 2012;23(3):206–208.
119. Gao M, Xu H, Zhang C, et al. Preparation and characterization of curcumin thermosensitive hydrogels for intratumoral injection treatment. *Drug Dev Ind Pharm*. 2014;40(11):1557–1564. doi:10.3109/03639045.2013.838579
120. Chen P, Zhang H, Cheng S, et al. Development of curcumin loaded nanostructured lipid carrier based thermosensitive in situ gel for dermal delivery. *Colloids Surfaces A*. 2016;506:356–362. doi:10.1016/j.colsurfa.2016.06.054

121. Chen D, Yu H, Mu H, et al. Novel chitosan derivative for temperature and ultrasound dual-sensitive liposomal microbubble gel. *Carbohydr Polym.* 2013;94(1):17–23. doi:10.1016/j.carbpol.2012.12.069
122. Cagel M, Tesan FC, Bernabeu E, et al. Polymeric mixed micelles as nanomedicines: achievements and perspectives. *Eur J Pharm Biopharm.* 2017;113:211–228. doi:10.1016/j.ejpb.2016.12.019
123. Biswas S, Kumari P, Lakhani PM, et al. Recent advances in polymeric micelles for anti-cancer drug delivery. *Eur J Pharm Sci.* 2016;83:184–202. doi:10.1016/j.ejps.2015.12.031
124. Yi Y, Lin G, Chen SY, et al. Polyester micelles for drug delivery and cancer theranostics: current achievements, progresses and future perspectives. *Mater Sci Eng C.* 2017;83(2):218–232. doi:10.1016/j.msec.2017.10.004
125. Zhang W, Cui T, Liu L, et al. Improving anti-tumor activity of Curcumin by polymeric micelles in thermosensitive hydrogel system in colorectal peritoneal carcinomatosis model. *J Biomed Nanotechnol.* 2015;11(7):1173–1182. doi:10.1166/jbn.2015.2073
126. Hu YF, Darcos V, Monge S, et al. Thermo-responsive release of curcumin from micelles prepared by self-assembly of amphiphilic P(NIPAAm-co-DMAAm)-b-PLLA-b-P(NIPAAm-co-DMAAm) triblock copolymers. *Int J Pharm.* 2014;476(1–2):31–40. doi:10.1016/j.ijpharm.2014.09.029

## International Journal of Nanomedicine

Dovepress

### Publish your work in this journal

The International Journal of Nanomedicine is an international, peer-reviewed journal focusing on the application of nanotechnology in diagnostics, therapeutics, and drug delivery systems throughout the biomedical field. This journal is indexed on PubMed Central, MedLine, CAS, SciSearch®, Current Contents®/Clinical Medicine,

Journal Citation Reports/Science Edition, EMBase, Scopus and the Elsevier Bibliographic databases. The manuscript management system is completely online and includes a very quick and fair peer-review system, which is all easy to use. Visit <http://www.dovepress.com/testimonials.php> to read real quotes from published authors.

Submit your manuscript here: <https://www.dovepress.com/international-journal-of-nanomedicine-journal>